IN THE UNITED STATES DISTRICT COURT
FOR THE DISTRICT OF DELAWARE

ZYMOGENETICS, INC., a Washington Corporation,	)	
Plaintiff,	)	Civil Action No: 06-500-SLR-MPT
v.	)	
BRISTOL-MYERS SQUIBB CO., a Delaware Corporation, and DOES 1 through 100,	)	**REDACTED PUBLIC VERSION**
Defendants.	)	

DECLARATION OF DANA LAU IN SUPPORT OF BRISTOL-MYERS SQUIBB COMPANY'S REPLY BRIEF FOR SUMMARY JUDGMENT OF NONINFRINGEMENT

I, Dana Lau, hereby declare the following:

1. I am an associate with the law firm of Fitzpatrick, Cella, Harper & Scinto, attorneys for Defendant Bristol-Myers Squibb Company ("Bristol") in this action. I submit this Declaration in support of Bristol's Reply Brief for Summary Judgment of Noninfringement.

2. Attached hereto as Noninfringement Reply Brief ("N.R.B.") Exhibit 1 is a true and correct copy of excerpts from Abatacept BMS-188667 Biologics Licensing Application (BMS001290162-163).

3. Attached hereto as N.R.B. Exhibit 2 is a true and correct copy of the Supplemental Expert Report of Jeffrey V. Ravetch, M.D., Ph.D.

4. Attached hereto as N.R.B. Exhibit 3 is a true and correct copy of the Supplemental Expert Report of John Kuriyan, Ph.D.

5. Attached hereto as N.R.B. Exhibit 4 is a true and correct copy of an excerpt of Peter Linsley Deposition Transcript at 39.

6. Attached hereto as N.R.B. Exhibit 5 is a true and correct copy of an excerpt of Jeffrey V. Ravetch Deposition Transcript at 165-166.

7. Attached hereto as N.R.B. Exhibit 6 is a true and correct copy of Orencia® (abatacept) An Alternative Treatment Option (BMS004294502-82).

8. Attached hereto as N.R.B. Exhibit 7 is a true and correct copy of Saphire et al. *Crystal Structure of a Neutralizing Human IgG Against HIV-1: A Template for Vaccine Design*, SCIENCE, 293:1155-59. (BMS001288355-59).

9. Attached hereto as N.R.B. Exhibit 8 is a true and correct copy of an excerpt of Kirk Leister Deposition Transcript at 51-52.

10. Attached hereto as N.R.B. Exhibit 9 is a true and correct copy of excerpts of Peter Linsley Deposition Transcript at 69-70, *The Regents of the University of Michigan v. Bristol-Myers Squibb Co.*, Case No. 73690 (E.D. Mich. May 19, 2001) (BMS004256349; BMS004256417-18).

11. Attached hereto as N.R.B. Exhibit 10 is a true and correct copy of Ikemizu et al. *Structure and dimerization of a soluble form of B7-1*, IMMUNITY, 12:51-60 (2000). (BMS001598144-53).

12. Attached hereto as N.R.B. Exhibit 11 is a true and correct copy of Davis et al., *A Murine T Cell Receptor Gene Complex. Isolation, Structure and Rearrangement*, IMMUNOLOGICAL REVIEWS, 81:235-258 (1984).

13. Attached hereto as N.R.B. Exhibit 12 is a true and correct copy of excerpts of David Ostrov Deposition Transcript at 44, 45, 48.

I declare under penalty of perjury under the laws of the United States of America that the foregoing is true and correct.

Executed this 25th day of August, 2008 in New York, New York.

Dana Lau

Exhibits 1-6 Redacted In Their Entirety

EXHIBIT 7

8. J. F. Partridge, B. Borgstrom, R. C. Allshire, *Genes Dev.* 14, 783 (2000).
9. X. Bi, J. R. Broach, *Curr. Opin. Genet. Dev.* 11, 199 (2001).
10. D. Donze, C. R. Adams, J. Rine, R. T. Kamakaka, *Genes Dev.* 13, 698 (1999).
11. S. I. S. Grewal, A. J. S. Klar, *Genetics* 146, 1221 (1997).
12. S. I. S. Grewal, *J. Cell. Physiol.* 184, 311 (2000).
13. G. Thon, A. Cohen, A. J. S. Klar, *Genetics* 138, 29 (1994).
14. N. Ayoub, I. Goldshmidt, A. Cohen, *Genetics* 152, 495 (1999).
15. J. Nakayama, J. C. Rice, B. D. Strahl, C. D. Allis, S. I. S. Grewal, *Science* 292, 110 (2001).
16. A. J. Bannister *et al.*, *Nature* 410, 120 (2001).
17. Chromatin immunoprecipitations were performed essentially as described (*7*, *8*). Fission yeast cells grown at 32°C in yeast extract adenine (YEA) medium (5 × 10⁸ cells at 10⁷ cells/ml for each reaction) were shifted to 18°C for 2 hours before 30-min fixation in 3% paraformaldehyde, and then were used to prepare soluble chromatin. Chromatin fractions were fragmented to ~0.5- to 0.8-kb DNA fragments before immunoprecipitation using antibodies to Swi6, H3 Lys⁹-methyl, or H3 Lys⁴-methyl. DNAs recovered from immunoprecipitated chromatin fractions or from whole-cell crude extracts were subjected to PCR analyses (94°C, 30 s; 55°C, 30 s; 72°C, 1 min; 30 cycles). PCR products were labeled by including 0.25 μl of [α-³²P]deoxycytidine triphosphate (10 mCi/ml) in each reaction; they were separated on a 4% polyacrylamide gel, and band intensities were quantified using a Fuji phosphoimager.
18. B. D. Strahl, C. D. Allis, *Nature* 403, 41 (2000).
19. T. Jenuwein, C. D. Allis, *Science* 293, 1074 (2001).
20. B. D. Strahl, R. Ohba, R. G. Cook, C. D. Allis, *Proc. Natl. Acad. Sci. U.S.A.* 96, 14967 (1999).
21. K. Takahashi, E. S. Chen, M. Yanagida, *Science* 288, 2215 (2000).
22. H. Wang *et al.*, *Science* 293, 853 (2001); published online 31 May 2001 (10.1126/science.1060781).
23. Because of recombination block in the silent mating-type region, replacement of IR-L or IR-R elements with *kan*ʳ was performed in the *swi6* mutant background, which allows recombination in this region. The DNA fragment containing the marker gene flanked by sequence corresponding to the 5′ or 3′ sequence of the site of integration was gel-purified and used for transformation to construct IR-R Δ and IR-L Δ strains. PCR and Southern analyses were used to confirm replacements. Genetic crosses were used to obtain *swi6*⁺ derivatives of the above strains. Deletions did not have a detectable effect on silencing of *ura4*⁺ (*Kint2::ura4*⁺) inserted at the *K*-region.
24. T. I. Cerasimova, K. Byrd, V. G. Corces, *Mol. Cell* 6, 1025 (2000).
25. H. N. Cai, P. Shen, *Science* 291, 493 (2001).
26. E. Muravyova *et al.*, *Science* 291, 495 (2001).
27. J. Nakayama, S. I. S. Grewal, unpublished data.
28. G. Thon, A. J. S. Klar, *Genetics* 134, 1045 (1993).
29. We thank J. Rice and E. Heard for comments on the manuscript, J. Nakayama for helpful discussions and boundary element sequences, and G. Xiao, Y. Tsukamoto, R. Rice, and M. A. Jelinek for technical help. Supported in part by a grant from Ellison Medical Foundation (S.I.S.G.) and by NIH grants GM59772 (S.J.S.G.) and GM53512 (C.D.A.).

6 July 2001; accepted 17 July 2001

Crystal Structure of a Neutralizing Human IgG Against HIV-1: A Template for Vaccine Design

Erica Ollmann Saphire,[1] Paul W. H. I. Parren,[2] Ralph Pantophlet,[2] Michael B. Zwick,[2] Garrett M. Morris,[1] Pauline M. Rudd,[4] Raymond A. Dwek,[4] Robyn L. Stanfield,[1] Dennis R. Burton,[1,2]* Ian A. Wilson[1,3]*

We present the crystal structure at 2.7 angstrom resolution of the human antibody IgG1 b12. Antibody b12 recognizes the CD4-binding site of human immunodeficiency virus–1 (HIV-1) gp120 and is one of only two known antibodies against gp120 capable of broad and potent neutralization of primary HIV-1 isolates. A key feature of the antibody-combining site is the protruding, finger-like long CDR H3 that can penetrate the recessed CD4-binding site of gp120. A docking model of b12 and gp120 reveals severe structural constraints that explain the extraordinary challenge in eliciting effective neutralizing antibodies similar to b12. The structure, together with mutagenesis studies, provides a rationale for the extensive cross-reactivity of b12 and a valuable framework for the design of HIV-1 vaccines capable of eliciting b12-like activity.

HIV-1 vaccine development is greatly hindered by the extreme difficulty in eliciting a neutralizing antibody response to the virus (*1*–*3*). However, three human monoclonal antibodies have been identified that can efficiently neutralize a broad array of primary isolates of HIV-1 in vitro (*4*) and can protect against viral challenge in vivo (*5*–*9*). Antibody 2F5 (*10*) reacts with gp41, whereas 2G12 (*11*) and b12 (*12*) react with independent epitopes on gp120. Elucidation of the epitopes recognized by these antibodies may offer valuable insights into the design of antigens capable of eliciting a protective antibody response.

Antibody b12 was identified from a combinatorial phage display library developed from bone marrow donated by a 31-year-old homosexual male who had been seropositive, but without symptoms, for 6 years (*12*). This antibody recognizes a highly conserved epitope overlapping the CD4-binding region of gp120, which accounts for its broad recognition of different HIV-1 isolates. Antibody b12 neutralizes about 75% of clade B primary viruses and a similar, or somewhat lesser, proportion of other clades (*12*, *13*). In addition, b12 can protect hu-PBL-SCID mice (*5*) and macaques (*7*) from viral challenge. This combination of potency and broad specificity suggests that the b12 epitope on gp120 may be a particularly effective target for vaccine design.

The b12 IgG1κ was expressed in CHO cells, purified, and crystallized as previously described (*14*). The crystal structure of the intact IgG1 was determined at 2.7 Å resolution through an exhaustive molecular replacement (MR) search using more than 100 individual Fc and Fab search models (*14*). The highly mobile hinge regions connecting the Fabs to the Fc domains were interpretable after extensive rebuilding, refinement, and density modification (Table 1). Only three residues of the upper hinge of one heavy chain, seven residues of a frequently disordered surface loop of one Fab C_{H1} domain (residues 128 to 135), and three COOH-terminal residues from one Fc are disordered.

The IgG structure is highly asymmetric (Fig. 1) and can be considered a "snapshot" of the broad range of conformations available in solution. The overall shape is between a Y and a T, with a 143° angle between the major axes of the two Fabs (*15*). The IgG spans 171 Å from the apex of one antigen-binding site to the other. The Fc region is twisted nearly perpendicularly to the planes of the Fabs and shifted some 32 Å from the central dyad relating the two Fabs, so that it packs into the space beneath only one of the Fabs (Fig. 1).

The hinge regions form extended structures with some conformational variation in torsion angles between the two chains, reflecting the different relative placement and environment of the two Fabs relative to the Fc domain. One upper hinge forms a spiral arrangement similar to a partially unwound helix; the other forms an extended turn as the polypeptide chain reverses direction to connect the Fab to the Fc. The core hinge region contains two adjacent pairs of cysteine residues, but only one disulfide is ob-

[1]Department of Molecular Biology, [2]Department of Immunology, [3]The Skaggs Institute for Chemical Biology, The Scripps Research Institute, 10550 North Torrey Pines Road, La Jolla, CA 92037, USA. [4]Department of Biochemistry, University of Oxford, The Oxford Glycobiology Institute, South Parks Road, Oxford OX1 3QU, UK.

*To whom correspondence should be addressed. E-mail: wilson@scripps.edu, burton@scripps.edu

Table 1. Structure determination of IgG1 b12. Data to 2.7 Å resolution were collected from a single cryocooled crystal at SSRL Beamline 7-1 on a MAR (MAR-Research) 30-cm area detector and processed with DENZO and SCALEPACK (*38*). Although the R_{sym} for the highest resolution shell is relatively high (62.6%), this shell contains useful information, because the I/σ is 2.4 and because inclusion of these reflections clearly improved the electron density maps. The structure was determined by molecular replacement (MR) using the software package AMoRe within the CCP4 suite (*39*) as described (*14*). Initial R_{cryst} and R_{free} values after MR and substitution of the b12 sequence were 0.37 and 0.44, respectively. The structure was refined in CNS (*40*) using a maximum likelihood target function and an initial overall anisotropic temperature factor correction. Multiple cycles of rebuilding in TOM/FRODO (*41*), refinement, as well as density modification in DM (*42*) by using a perturbation-γ correction, dramatically clarified density and allowed construction of approximately 65 residues in the hinge, carbohydrate, and solvent-exposed regions. The overall average *B* value is 90 Å², reflecting the high solvent content of the crystals and interdomain flexibility of the IgG molecule. However, the electron density, with exception of the flexible hinge region and some solvent exposed loops, is absolutely clear and completely unambiguous. Water molecules were only built into highly ordered regions of the structure. *B* values for protein atoms in the vicinity of the incorporated water molecules ranged from 30 to 65 Å².

Parameter	Value
Data collection	
Space group	R32
Unit cell dimensions (Å)	$a = b = 271.3$, $c = 175.2$
Matthew's coefficient (V_M, Å³Da⁻¹)	4.1, 70% solvent
Resolution	30–2.7 Å
Total observations	187712 (8424)*
Unique reflections	63686 (3113)*
R_{sym} (%)	7.2 (62.6)*
Completeness (%)	94.4 (95.5)*
Redundancy	2.9 (2.7)*
I/σ	17.6 (2.4)*
Refinement	
Total residues	1331
Water molecules	71
Sugars	18
Refinement range (Å)	30–2.7
R_{cryst} (%)	22.5
R_{free} (%)	27.2
Bond length deviation (Å)	0.005
Bond angle deviation (°)	1.2
Residues in most favored regions (%) of Ramachandran plot	89.7
Residues in disallowed regions (%)	0.2†
Average *B* value, protein (Å²)	90
Average *B* value, water (Å²)	58
Average *B* value, carbohydrate (Å²)	142

*Values for outer shell from 2.75 to 2.70 Å. †Val³³ of both light chains. This residue exists in a well-defined γ turn in almost all antibody structures, but is designated by PROCHECK (*43*) as an outlier.

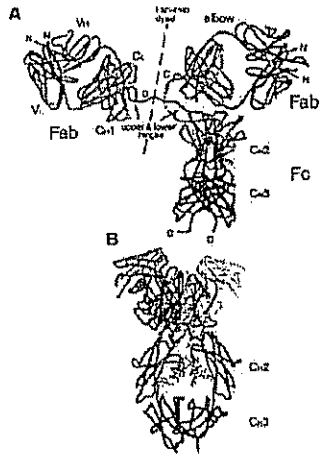


Fig. 1. Cα trace of the intact human IgG1 b12. The residues are colored by B value, with lower than average colored blue, average colored white, and higher than average colored red. (A) Front view showing the reach of the two Fabs and packing of the Fc domain underneath the right Fab. The hinge regions and one Fc C_H2 are characterized by the highest B values and greatest mobility. (B) Side view of the IgG [rotated 90° from (A)] demonstrating the near-perpendicular twist of the Fc relative to the Fabs. Carbohydrate chains form the contact between the C_H2 domains and are illustrated in ball-and-stick. Figure generated with Bobscript (*44*) and Raster3D (*45*). See (*46*) for an interactive image.

served in the electron density maps. The broken disulfide may be dynamic or may be a result of radiation damage, but probably has no functional importance, as only a single hinge disulfide is necessary for complement-mediated lysis and antibody-dependent cell-mediated cytotoxicity and phagocytosis (*16*).

Carbohydrate sequencing of b12 reveals two biantennary-branched oligosaccharide chains, but with branching fucose and terminal galactose residues in incomplete occupancy (*14*). This asymmetry is reflected in the electron density maps where one chain has both terminal galactose residues but lacks the fucose; the other incorporates the fucose but lacks the terminal galactose on the 1,3 arm.

Antibody b12 has a long CDR H3 (18 amino acids) that rises 15 Å above the surface of the antigen-binding site with a Trp residue at its apex (Fig. 2). A patch of acidic residues (*17*) along one face of this loop may help maintain the vertical projection through charge repulsion. This extended CDR H3 finger-like loop would allow the antibody to probe the recessed CD4-binding site of gp120; all members of a panel of 32 antibodies against the CD4-binding site developed from phage display have a similar length CDR H3 (*18*). To validate this notion, we designed a synthetic peptide to mimic the crystal structure of CDR H3. The peptide by itself is capable of viral neutralization when coupled to bovine serum albumin (BSA) (*19*) (Fig. 3).

Traditional views suggest that antigen-binding sites for antibodies against proteins are relatively flat. However, extended H3 loops are frequently seen in human antibodies directed against pathogens (*20*–*22*) that would allow them to access canyons and clefts on the viral surface (*23*). It is noteworthy that mouse antibodies do not normally exhibit such long CDR H3 loops, and indeed, few murine antibodies against the CD4-binding site have been described relative to the corresponding plethora of human antibodies of this specificity.

Ideally, we would prefer to dock our b12 structure onto an envelope gp120 trimer, as this is probably the relevant structure for neutralization. However, the only available gp120 structure is that of its monomeric core as a complex with CD4 and a Fab fragment (*24*). One interpretation of thermodynamic studies on recombinant monomeric gp120 is that CD4 binding might be accompanied by some structural rearrangement in gp120 (*25*). However, because structures of core gp120 from a primary isolate and a T cell line–adapted virus can be superimposed (*24*, *26*) and because earlier studies indicated that b12 and CD4 are sensitive to the same mutations in gp120, it is reasonable to use the CD4-bound core gp120 structure for generation of a docking model that can be tested by mutagenesis.

One hundred computational docking experiments were performed in parallel by using AutoDock (*27*). Each experiment used a 126 × 126 × 126 Å grid centered on gp120, each using 250,000 energy evaluations, and different, randomly selected initial orientations and translations of the b12 Fv. The best

Approved 1.0 saphire2001.pdf
onfidential BMS 001288356

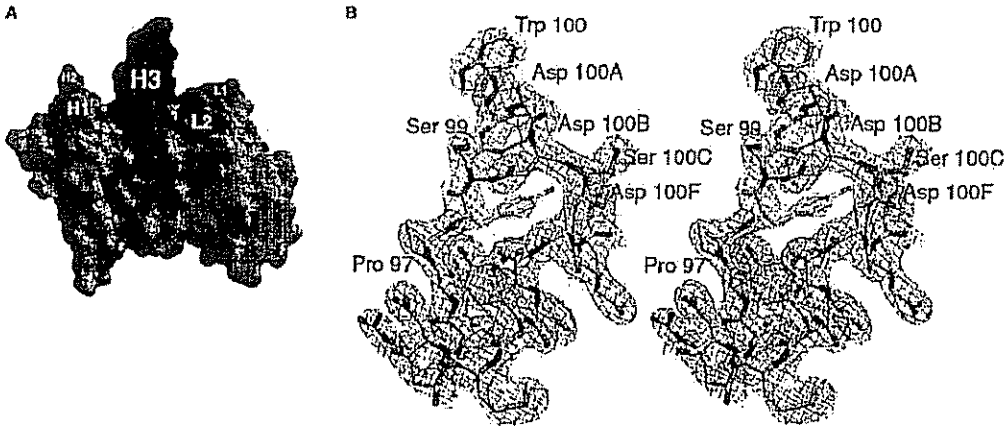


Fig. 2. Prominence of the CDR H3 finger-like loop in IgG1 b12. (A) Side view of the antigen-binding site of the Fv portion of b12. Contributions to the surface from each CDR are indicated. CDR H3 projects 15 Å above the other CDRs. (B) Stereo view of CDR H3 with surrounding final $2F_{obs} - F_{calc}$ electron density contoured at 2.0 σ. Trp^{100} is presented at the apex of the loop, and five intra-loop hydrogen bonds are indicated by dotted blue lines. The CDR H3 is unlikely to deform upon gp120 binding because of the presence of aromatic residues at the base and charge repulsion of the acidic patch on the inner face. In fact, four crystallographically distinct structures of the CDR H3 are identical [two on this symmetric IgG and two solved as Fab fragments in complex with a peptide (*47*)]. Molecular surfaces were calculated by using MSMS (*48*) and a 1.5 Å probe and visualized by using PMV (*49*). Density figure generated by using Bobscript (*44*) and Raster3D (*45*).

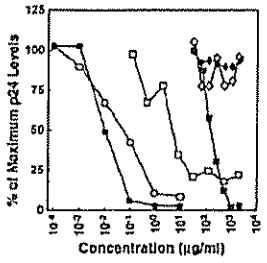


Fig. 3. Neutralization of HIV-1_{MN} and HIV-1_{HxB2} by IgG1 b12 and by a synthetic CDR H3 peptide. The peptide was designed as a CDR H3 loop mimic and coupled to BSA. A control peptide Gβ (American Peptide Co., Inc.) does not neutralize when coupled to BSA. HIV-1_{MN} and HIV-1_{HxB2} were neutralized by using H9 target cells and detection of p24 in ELISA as a reporter assay as described in (*5*). Filled circles, IgG1 b12 (MN); open circles, IgG1 b12 (HxB2); filled squares, CDR H3-BSA (MN); open squares, CDR H3-BSA (HxB2); filled diamonds, Gβ-BSA (MN); open diamonds, Gβ-BSA (HxB2).

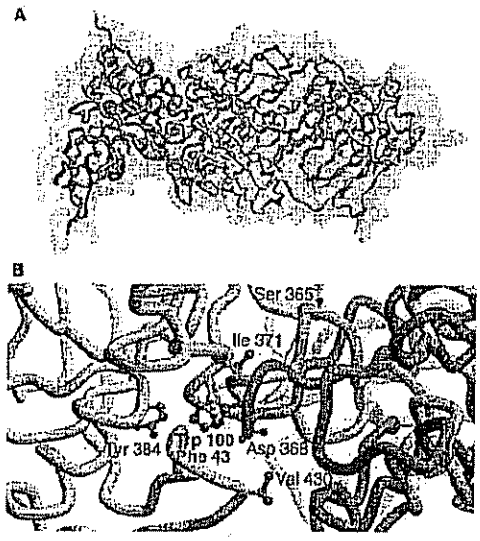


Fig. 4. Model of b12 interacting with gp120. (A) Comparison of Fab b12 docking onto gp120 with the CD4-gp120 crystal structure (*24*). Fab b12 is drawn as a Cα trace in yellow and gp120 in gray, showing the high complementarity of the gp120 and b12 structures, with their corresponding molecular surfaces outlined in the background. The placement of b12 overlaps with that of CD4 (red). (B) Close-up view of the docking. The b12 antibody presents Trp^{100} at the apex of the extended CDR H3 into the same pocket on gp120 that would be occupied by Phe^{43} of CD4 (red). Several gp120 residues (Ser^{365}, Asp^{368}, Ile^{371}, Tyr^{384}, and Val^{430}) that are important to b12 binding are illustrated in gray.

docking model has an energy of −24.7 kcal/mol, which is comparable to those obtained when docking CD4 onto gp120 in which AutoDock recreated the crystallized CD4-gp120 complex (*28*). This computational docking (Fig. 4A) arrives at a solution essentially identical to that first obtained manually, by using physical models generated from the b12 and gp120 coordinates.

The crystal structure of the gp120 complex (*24*, *26*) demonstrates that CD4 inserts a loop terminating in Phe^{43} into a polar pocket in gp120 in order to achieve complementarity (Fig. 4B). An antibody is twice as wide as CD4 (two immunoglobulin domains in width versus one). Thus, the imprint of a Fab onto the neutralizing face of gp120 will be extremely limited by geometric fit. The opening of the CD4-binding face of gp120 between the V1/V2 loop stem and constant region 4 (C4) is 35 Å wide, whereas the width of the Fab combining site is 31 Å. For gp120 in the envelope trimer, space for b12 binding in the lateral direction is bounded by the trimer interface and the 2G12 epitope, as b12 can bind native trimeric spikes (*29*), and also bind gp120

concurrently with antibody 2G12 (*30*). The docking shows that b12 may fit snugly onto gp120 by binding an epitope extending from the V1/V2 loop stem across the neutralizing face, with Trp^{100} at the tip of the H3 loop penetrating the Phe^{43} pocket (Fig. 4B). Trp^{100} is a crucial residue for b12 binding to gp120, as it is exclusively selected when CDR H3 residues are randomized (*31*). Further, mutation to Phe diminishes binding by 50% under conditions for which mutation to Ala, Val, or Ser diminishes binding by 85% (*32*).

IgG1 b12 and gp120 demonstrate complementary contact surfaces, like fingers fitting into a glove (Fig. 4A). The protruding ridge formed by Ser^{364} through Asp^{368} fits into a cleft between CDRs H3 and H2, and the protruding D loop of gp120 fits into a depression formed between CDRs H3, L1, and L3. In the docking model, approximately 2070 $Å^2$ of solvent-accessible surface is buried in the b12-gp120 interface (1030 $Å^2$ on gp120 and 1040 $Å^2$ on b12). The b12 interaction surface, like the footprint of CD4, is centered on the outer domain of gp120 with some additional contact extending to the V1/V2 loop stem, but with minimal contact to the inner domain.

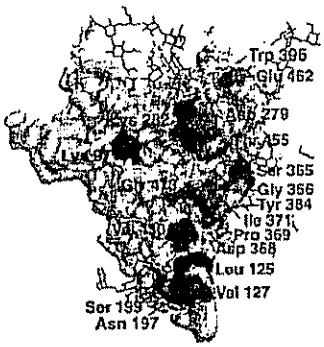


Fig. 5. Validation of the docking model of b12 onto gp120. Results of point mutations suggested by docking of b12 onto gp120 were mapped onto the gp120 surface. Mutation of residues in blue enhances b12 binding (>200% affinity relative to wild type); mutations in red diminish b12 binding (<50% relative affinity); and mutations in black have no significant effect (between 50 and 200% relative affinity). Most mutations are in the outer domain of gp120; see (*46*) for full characterization of mutants. The docking footprint of b12 on gp120 is outlined with a dashed black line. Variants of HIV-1 clade B isolates that escape neutralization by b12 have been generated in vitro (*50*) and in vivo (*51*). A common feature of these neutralization escape variants is the mutation of a proline at position 369, which strongly reduces b12 binding to gp120 in clade B isolates (*50*). Hence, Pro^{369} has been indicated with hatched red lines in this figure. Figure generated in PMV (*49*)

From this docking, a list of likely contact residues was generated. Alanine mutation of seventeen of these and additional neighboring residues supports the docking model (Fig. 5). In fact, several mutations enhance b12 binding, suggesting that b12, like CD4, may recognize gp120 through many main-chain contacts, allowing b12 to be relatively insensitive to side-chain variation.

The ability of b12 to neutralize primary viruses is associated with its ability to bind trimeric, as well as monomeric, gp120, whereas the other noncneutralizing CD4-binding site antibodies principally bind only monomeric gp120. Antibody b12 is also unique in its sensitivity to mutations associated with the V1/V2 loop (*29*) and, in particular, to changes in the V2 stem structure (*33*). In our model, the b12 Fab fits onto gp120 by contacting the inside face of the V1/V2 loop stem. We suggest that this mode of interaction angles the rest of the antibody bulk away from the trimer interface in an arrangement that permits attachment to the oligomeric spikes on the viral surface. Thus, the likely reason that antibody b12 is capable of potent neutralization of a broad array of isolates is that its interaction with the conserved CD4 epitope is mediated through many main-chain contacts and is angled in such a way that the antibody can access its epitope on the native viral surface.

Trimeric envelope spikes have three equivalent CD4-binding sites. Although the 170 Å reach of the IgG indicates that it could bivalently span two different spikes (*34*), b12 would probably not be able to bind simultaneously to two binding sites on the same trimeric spike. Nevertheless, the large mass (150 kD) of the IgG molecule compared with that of the envelope trimer is likely to block attachment of the virus to the target cell and/or fusion of viral and cell membranes, even at coating densities well below three IgG molecules per trimeric spike (*35*).

In conclusion, the structure of an intact human antibody capable of neutralizing a broad range of primary HIV-1 isolates illuminates the surface topography of the antigen-binding site. The highly extended CDR H3 is capable of accessing the vulnerable CD4-binding site of gp120 and may provide leads for antiviral compounds or peptides. Fine mapping of the b12 epitope also facilitates the design of minimized gp120 cores or peptidomimetics. Such structural information should provide new possibilities in the global effort to design an effective HIV-1 vaccine.

References and Notes:

1. R. Wyatt, J. Sodroski, *Science* 280, 1884 (1998).
2. D. R. Burton, *Proc. Natl. Acad. Sci. U.S.A.* 94, 10018 (1997).
3. P. W. H. I. Parren, J. P. Moore, D. R. Burton, Q. J. Sattentau, *AIDS* 13 (suppl. A), S137 (1999).
4. M. P. D'Souza, D. Livnat, J. A. Bradac, S. H. Bridges, *J. Infect. Dis.* 175, 1056 (1997).
5. M. C. Gauduin *et al.*, *Nature Med.* 3, 1389 (1997).
6. J. R. Mascola *et al.*, *Nature Med.* 6, 207 (2000).
7. P. W. H. I. Parren *et al.*, *J. Virol.* 75, 8340 (2001).
8. T. W. Baba *et al.*, *Nature Med.* 6, 200 (2000).
9. J. R. Mascola *et al.*, *J. Virol.* 73, 4009 (1999).
10. T. Muster *et al.*, *J. Virol.* 67, 6642 (1993).
11. A. Trkola *et al.*, *J. Virol.* 70, 1100 (1996).
12. D. R. Burton *et al.*, *Science* 266, 1024 (1994).
13. A. Trkola *et al.*, *J. Virol.* 69, 6609 (1995).
14. E. O. Saphire, P. W. H. I. Parren, C. F. Barbas, D. R. Burton, I. A. Wilson, *Acta Crystallogr. D57*, 168 (2001).
15. Definitions of axes used to quantify rotational and translational asymmetry. A central dyad was defined by the rotation axis that relates one Fab to the other Fab. One Fab is translated 16 Å from the other along the dyad (translation defined by the intersections of the Fab major axes with that dyad). The three axes within each domain (major, minor, and depth) are defined as follows: A major axis, extending from the hinge attachment point at the COOH-terminus to the center of the antigen-binding site was defined by the pseudo-dyad relating the C_H1 to C_L subdomains in the Fabs and the dyad relating the C_H3 subdomains in the Fc. The minor axis was defined as perpendicular to the major axis and extending across the flexible switch regions between the variable and constant domains of the Fabs (roughly across residues 107 of the light chain and 113 of the heavy chain) and across the switch region connecting the C_H2 to C_H3 domain of the Fc. The depth axes extend in the third dimension perpendicularly to both the major and minor axes. The 180° rotation of one Fab relative to the other refers to the rotation between the two depth axes of the two Fabs. Fab elbow angles are defined as the angle of intersection of the pseudo-dyad relating C_H1 and C_L with the pseudo-dyad relating V_H and V_L. The elbow angles (170°, 174°) differ slightly between the two Fabs. The Fc elbow angle, defined by the intersection of the dyad relating the C_H3 domains with the dyad relating the C_H2 domains, is 175°, revealing some asymmetry in the two halves of the Fc.
16. T. E. Michaelsen *et al.*, *Proc. Natl. Acad. Sci. U.S.A.* 91, 9243 (1994).
17. Asp 100A, Asp 100B, Asp 100F, Ser 99, Ser 100C, and Tyr 100L. Alanine mutation of any of the three Asp residues along this face results in weaker binding to $gp120_{BaL}$ (*32*).
18. All of the clones, with one exception, have a CDR H3 length of 18 to 22 residues (*21*), which is in marked contrast to the normal variation seen in other human antibodies (*36*). Antibodies to other HIV-1 epitopes have CDR H3 lengths ranging between 4 and 18 residues. The long length is not a function of their generation from a combinatorial library, because similar libraries of human antibodies against other pathogens display great variation in CDR length.
19. A synthetic peptide mimic of the CDR H3 was designed on the basis of the b12 crystal structure. The peptide extends from Ala^{93} to Trp^{103} and is linked at the base through native chemical ligation (*37*) and a Pro-Gly-Lys to promote type II β turn formation (sequence: C-PGK-ARVGPYSWDDSPQDNYYMDVW). The peptides were coupled to activated BSA (Pierce) through linkage with the cysteine residue at the base of the loop. Activity of the CDR H3 peptide was compared to that of b12 and of a control peptide similarly linked to BSA (GTP-binding peptide of sequence CEGNVRSELAGHTGV; American Peptide Co.). The peptide neutralizes $HIV\text{-}1_{IIIB}$ and $HIV\text{-}1_{MN}$. As expected, a higher concentration of the synthetic CDR H3 is required compared to the parental antibody that contains all six CDRs. HxB2 is a molecular clone of the HIV-1 strain IIIB. Single-letter abbreviations for the amino acids are as follows: A, Ala; C, Cys; D, Asp; E, Glu; F, Phe; G, Gly; H, His; I, Ile; K, Lys; L, Leu; M, Met; N, Asn; P, Pro; Q, Gln; R, Arg; S, Ser; T, Thr; V, Val; W, Trp; and Y, Tyr.
20. R. Kunert, F. Rüker, H. Katinger, *AIDS Res. Hum. Retrovir.* 14, 1115 (1998).
21. C. F. Barbas *et al.*, *J. Mol. Biol.* 230, 812 (1993).
22. P. P. Sanna, R. A. Williamson, A. De Logu, F. E. Bloom, D. R. Burton, *Proc. Natl. Acad. Sci. U.S.A.* 92, 6439 (1995).
23. T. J. Smith, E. S. Chase, T. J. Schmidt, N. H. Olson, T. S. Baker, *Nature* 383, 350 (1996).
24. P. D. Kwong *et al.*, *Nature* 393, 648 (1998).

onfidential BMS 001288358

25. D. G. Myszka *et al.*, *Proc. Natl. Acad. Sci. U.S.A.* **97**, 9026 (2000).
26. P. D. Kwong *et al.*, *Structure Fold. Des.* **8**, 1329 (2000).
27. G. M. Morris *et al.*, *J. Comp. Chem.* **19**, 1639 (1998).
28. AutoDock 3.0.5 was used to perform all protein-protein docking experiments by using the Lamarckian Genetic Algorithm (*27*). AutoGrid chemical affinity and electrostatics maps were computed and centered on gp120 with 126 × 126 × 126 grid points at a spacing of 1 Å. As a test of the method, AutoDock was able to dock the D1 domain of CD4 onto gp120 to recreate the crystallized complex of CD4 and gp120 to within 0.5 Å root mean square (rms) deviation. For CD4-gp120 docking, correct solutions clustered together at about −21 kcal/mol, whereas the next lowest energy solutions were about −11 kcal/mol. In order to reduce the number of atoms in the large b12-gp120 docking experiment, we docked only the Fv domain instead of the intact IgG. The two lowest energy dockings could be ruled out because the antibody constant domains overlapped gp120 when the full antibody was reconstructed from the Fv fragment. The next four lowest energy dockings formed the largest cluster, and had a median rms deviation of 2.3 Å from the initial model generated by hand from geometric constraints. This initial model complex was solvated by a 5 Å shell of water molecules and energy minimization performed by using the Discover 3 module of Insight II 2000 package (Molecular Simulations, San Diego, CA) and the CVFF force field for 100 iterations. This short minimization was enough to relieve any close contacts. Docking of the minimized structures resulted in a large 11-member cluster of solutions, with an average energy of −24.7 kcal/mol, unambiguously separated in energy from the remaining solutions.
29. P. Roben *et al.*, *J. Virol.* **68**, 4821 (1994).
30. J. P. Moore, J. Sodroski, *J. Virol.* **70**, 1863 (1996).
31. W. P. Yang *et al.*, *J. Mol. Biol.* **254**, 392 (1995).
32. M. B. Zwick *et al.*, unpublished data.
33. J. M. Binley *et al.*, *AIDS Res. Hum. Retrovir.* **14**, 191 (1998).
34. H. R. Gelderblom, E. H. Hausmann, M. Ozel, G. Pauli, M. A. Koch, *Virology* **156**, 171 (1987).
35. D. R. Burton, E. O. Saphire, P. W. H. I. Parren, *Curr. Top. Microbiol. Immunol.* **260**, 109 (2001).
36. I. Sanz, *J. Immunol.* **147**, 1720 (1991).
37. P. E. Dawson, T. W. Muir, I. Clark-Lewis, S. B. Kent, *Science* **266**, 776 (1994).
38. Z. Otwinowski, W. Minor, *Methods Enzymol.* **276**, 307 (1997).
39. J. Navaza, *Acta Crystallogr.* **A50**, 157 (1994).
40. A. T. Brünger *et al.*, *Acta Crystallogr.* **D54**, 905 (1998).
41. T. A. Jones, in *Computational Crystallography*, D. Sayre, Ed. (Oxford Univ. Press, Oxford, 1982), pp. 303–317.
42. K. D. Cowtan, P. Main, *Acta Crystallogr.* **D52**, 43 (1996).
43. R. A. Laskowski, M. W. MacArthur, D. S. Moss, J. M. Thornton, *J. Appl. Crystallogr.* **26**, 283 (1993).
44. R. M. Esnouf, *Acta Crystallogr.* **D55**, 938 (1999).
45. E. A. Merritt, D. J. Bacon, *Methods Enzymol.* **277**, 505 (1997).
46. Supplementary material is available in *Science* Online at www.sciencemag.org/cgi/content/full/293/5532/1155/DC1.
47. E.O.S., M.B.Z., A. Menendez, P.W.H.I.P., D.R.B., J. K. Scott, and I.A.W., unpublished observations.
48. M. F. Sanner, A. J. Olson, J. C. Spehner, *Biopolymers* **38**, 305 (1996).
49. M. F. Sanner, *J. Mol. Graph. Mod.* **17**, 57 (1999).
50. H. Ma *et al.*, *J. Virol.* **71**, 6869 (1997).
51. P. Polgnard *et al.*, *Immunity* **10**, 431 (1999).

52. Supported by NIH Grants GM46192 (I.A.W.), AI40377 (P.W.H.I.P.), and AI33292 (D.R.B.). We are extremely grateful to the staff of the Stanford Synchrotron Radiation Laboratory (SSRL) Beamline 7-1 for assistance in data collection, M. Wormald of the Oxford Glycobiology Institute (UK) for discussions of carbohydrate torsion angles, A. de Vos of Genentech for human Fc coordinates, J. Sodroski of Harvard University for plasmid pSVIIIenv, V. Roberts for discussions of electrostatics and docking, P. Dawson for peptide synthesis, P. Polgnard for help with gp120 mutagenesis, and M. Wang and A. Hessell for technical assistance. This is publication 13874-MB from The Scripps Research Institute. The IgG1 b12 coordinates and structure factors have been deposited into the Protein Databank (PDB accession code 1HZH) and are available from wilson@scripps.edu.

17 April 2001; accepted 18 June 2001

Enforcement of Temporal Fidelity in Pyramidal Cells by Somatic Feed-Forward Inhibition

Frédéric Pouille and Massimo Scanziani*

The temporal resolution of neuronal integration depends on the time window within which excitatory inputs summate to reach the threshold for spike generation. Here, we show that in rat hippocampal pyramidal cells this window is very narrow (less than 2 milliseconds). This narrowness results from the short delay with which disynaptic feed-forward inhibition follows monosynaptic excitation. Simultaneous somatic and dendritic recordings indicate that feed-forward inhibition is much stronger in the soma than in the dendrites, resulting in a broader integration window in the latter compartment. Thus, the subcellular partitioning of feed-forward inhibition enforces precise coincidence detection in the soma, while allowing dendrites to sum incoming activity over broader time windows.

At certain brain synapses, reliable transmission is ensured through large, rapidly rising, excitatory postsynaptic potentials (EPSPs), which are able to trigger a spike with little latency variation (*1*).

In hippocampal pyramidal cells (PCs), the small size of most unitary EPSPs requires that synaptic activity summate to reach the spike threshold (*2*). In principle, the relatively long membrane time constant of these neurons (*3*) may allow EPSPs to summate over large time windows. The occurrence of spikes would then reflect the average synaptic bombardment over time instead of being selectively time-locked to coincident synaptic activity. Thus, it is not known whether the timing of a spike in PCs reports the timing of the afferent activity triggering the spike (*4*–*6*). This issue can be addressed experimentally by determining the time window within which the activity of independent synaptic inputs must occur to trigger a spike.

We recorded from CA1 PCs in acute hippocampal slices from rat brains in cell-attached mode to avoid interfering with the intracellular ionic composition. Two stimulation electrodes were placed in the stratum radiatum at 300 to 600 μm on each side of the recorded neuron (*7*). Stimulation intensity was set so that when the two Schaffer collateral pathways were stimulated simultaneously, the PC fired a spike, detected as a capacitive current, in about 50% of the trials (threshold stimulation). The probability of spiking steeply decreased when one of the stimuli was shifted in time in 2.5- or 5-ms steps (Fig. 1A). A Gaussian fit of the data gave a SD of 1.4 ms (n = 9 cells).

We then blocked γ-aminobutyric acid A receptors ($GABA_AR$) with bicuculline (20 μM) or with the more selective antagonist SR95531 (3 μM) (*8*) and readjusted the stimulation intensity of both pathways to match the spiking probability observed under control conditions with simultaneous stimulation (51 ± 3% in control conditions versus 50 ± 5% in the presence of bicuculline, n = 5 cells; 62 ± 6% in control conditions versus 64 ± 11% in the presence of SR95531, n = 4 cells). This increased the delay between stimulus and spike (8.2 ± 0.6 ms in control conditions, 16.8 ± 1.2 ms in the presence of $GABA_AR$ antagonist; n = 9 cells).

$GABA_AR$ antagonists greatly prolonged the integration window (SD = 17.8 ms in bicuculline, n = 5 cells; SD = 15.6 ms in SR95531, n = 4 cells). In addition, although spikes triggered with simultaneous stimulation under control conditions showed submillisecond variability in spike delay (jitter), as described for intracellular current injections (*9*), in the presence of $GABA_AR$ antagonists the jitter increased almost threefold (the SD was 0.5 ms in control conditions versus 1.4 ms with $GABA_AR$ antagonists, n = 9 cells; Fig. 1B).

We monitored the underlying synaptic events using whole-cell recordings. In voltage-clamped cells, a stimulus elicited an excitatory postsynaptic current (EPSC)–inhibi-

Brain Research Institute, University of Zürich, Winterthurerstrasse 190, CH-8057 Zürich, Switzerland.

*To whom correspondence should be addressed. E-mail: massimo@hifo.unizh.ch

onfidential BMS 001288359

Exhibit 8
Redacted In Its Entirety

Exhibit 9
Redacted In Its Entirety

EXHIBIT 10

Immunity, Vol. 12, 51–60, January, 2000, Copyright ©2000 by Cell Press

Structure and Dimerization of a Soluble Form of B7-1

Shinji Ikemizu,* Robert J. C. Gilbert,*‡
Janet A. Fennelly,† Alison V. Collins,† Karl Harlos,*‡
E. Yvonne Jones,*‡ David I. Stuart,*‡§
and Simon J. Davis†§
*Division of Structural Biology
Wellcome Trust Centre for Human Genetics
The University of Oxford
Roosevelt Drive
Oxford OX3 7BN
United Kingdom
†Nuffield Department of Clinical Medicine
The University of Oxford
John Radcliffe Hospital
Headington, Oxford OX3 9DU
United Kingdom
‡Oxford Centre for Molecular Sciences
The University of Oxford
New Chemistry Laboratory
South Parks Road
Oxford OX1 3QT
United Kingdom

Summary

B7-1 (CD80) and B7-2 (CD86) are glycoproteins expressed on antigen-presenting cells. The binding of these molecules to the T cell homodimers CD28 and CTLA-4 (CD152) generates costimulatory and inhibitory signals in T cells, respectively. The crystal structure of the extracellular region of B7-1 (sB7-1), solved to 3 Å resolution, consists of a novel combination of two Ig-like domains, one characteristic of adhesion molecules and the other previously seen only in antigen receptors. In the crystal lattice, sB7-1 unexpectedly forms parallel, 2-fold rotationally symmetric homodimers. Analytical ultracentrifugation reveals that sB7-1 also dimerizes in solution. The structural data suggest a mechanism whereby the avidity-enhanced binding of B7-1 and CTLA-4 homodimers, along with the relatively high affinity of these interactions, favors the formation of very stable inhibitory signaling complexes.

Introduction

The course of an immune response is in large part controlled by the interactions of leukocyte cell surface molecules. Among the most important are those involving the B7 molecules B7-1(CD80) and B7-2(CD86), which are expressed on antigen-presenting cells and bind to both CD28 and CTLA-4(CD152) expressed on T cells (reviewed by Lenschow et al., 1996; Greenfield et al., 1998). Altering these interactions has profound effects on immune responses in experimental disease models. Enhanced anti-tumor immune responses result from transfecting B7-1 into murine tumors (Chen et al., 1992; Townsend and Allison, 1993) or from using anti-CTLA-4 antibodies to block CTLA-4 interactions with B7-1 and B7-2 (Leach et al., 1996). Conversely, inhibition of B7/CD28 interactions results in general immunosuppression (Linsley et al., 1992b), reduced autoantibody production (Finck et al., 1994), and enhanced skin and cardiac allograft survival (Larsen et al., 1996). There is, therefore, considerable interest in the therapeutic potential of manipulating human B7 interactions, and such approaches have already shown promise (Guinan et al., 1999).

B7-1 and B7-2 each consist of single V-like and C-like immunoglobulin superfamily (IgSF) domains (Freeman et al., 1989, 1993a; Azuma et al., 1993). Their ligands, CD28 and CTLA-4, are also structurally related and are expressed at the cell surface as homodimers of single V-like IgSF domains (Aruffo and Seed, 1987; Brunet et al., 1987). A third CD28-like molecule, ICOS (Hutloff et al., 1999), interacts with another B7-related molecule (D. Brodie et al., unpublished data), but the analysis of transgenic mice indicates that B7-1 and B7-2 are the only functional ligands of CD28 and CTLA-4 (Mandelbrot et al., 1999). The affinities of these interactions differ substantially: human CTLA-4 binds B7-1 with a solution K_d of 0.2–0.4 μM (van der Merwe et al., 1997), whereas the affinity of CD28 for B7-2 is 40- to 100-fold lower (B7-1/CD28 and B7-2/CTLA-4 interactions each have intermediate affinities [K_d = 4 μM]; A. V. C. et al., unpublished data).

The expression of B7-1, B7-2, CD28, and CTLA-4 is tightly regulated: whereas CD28 is constitutively expressed on resting human T cells and B7-2 is rapidly induced on antigen-presenting cells early in immune responses, the expression of both B7-1 and CTLA-4 is considerably delayed (reviewed by Lenschow et al., 1996). Interactions of the B7 molecules with CD28 generate costimulatory signals amplifying T cell receptor (TCR) signaling and preventing anergy, whereas interactions with CTLA-4 induce powerful inhibitory signals in T cells (Martin et al., 1986; Weiss et al., 1986; Harding et al., 1992; Walunas et al., 1994; Waterhouse et al., 1995). CD28-dependent costimulation is poorly understood, but recent work implicates the bulk recruitment of cell surface molecules and kinase-rich rafts to the site of TCR engagement, favoring receptor phosphorylation and signaling (Viola et al., 1999; Wülfing and Davis, 1999). Conversely, CTLA-4 inhibits signal transduction by recruiting the tyrosine phosphatase SHP-2 to the TCR, resulting in dephosphorylation of the ζ chain of the complex and components of the RAS signaling pathway (Marengere et al., 1996; Lee et al., 1999), and by interfering with distal events in the CD28 signaling pathway (Olsson et al., 1999).

While the opposing effects of CD28 and CTLA-4 are clear cut, distinct functions for B7-1 and B7-2 have yet to be defined. A role in TH_0, TH_1, or TH_2 differentiation has been proposed (Freeman et al., 1995; Kuchroo et al., 1995), but other work (Schweitzer et al., 1997) suggests that B7-1 and B7-2 determine the magnitude of

§To whom correspondence should be addressed (e-mail: david.stuart@strubi.ox.ac.uk and sdavis@molbiol.ox.ac.uk).

costimulatory signals rather than the outcome of TH subset differentiation (reviewed by McAdam et al., 1998). Supporting this view, quantitative rather than qualitative effects on tyrosine phosphorylation follow the stimulation of T cells with artificial antigen-presenting cells expressing B7-1 or B7-2 (Slavik et al., 1999). Moreover, gene disruption studies reveal considerable overlap in the costimulatory functions of B7-1 and B7-2 (Freeman et al., 1993b; Borriello et al., 1997). A third possibility is that, rather than having distinct CD28-dependent costimulatory roles, the key functional differences concern the strength and/or mode of binding of B7-2 and B7-1 to CD28 and CTLA-4.

We have determined the crystal structure of a soluble (s) form of human B7-1 at 3 Å resolution. The structure of the sB7-1 monomer combines features of both the adhesion and antigen receptor subgroups of the IgSF. The arrangement of sB7-1 monomers in the crystal lattice implies that sB7-1 might spontaneously form homodimers, an observation we confirm using analytical ultracentrifugation. These results have important implications regarding the structure and properties of the signaling complexes B7-1 will form in the contact zones between antigen-presenting cells and T cells.

Results

Structure Determination

A histidine-tagged, selenomethionine (SeMet)-labeled form of sB7-1 consisting of residues 1–201 of the mature polypeptide (van der Merwe et al., 1997) was expressed in the Chinese hamster–derived, Lec3.2.8.1 cell line in the presence of 0.5 mM N-butyl deoxynojirimycin and then deglycosylated as described (Butters et al., 1999). Deglycosylated, unlabeled sB7-1 bound CTLA-4 with wild-type affinity (A. V. C. et al., unpublished data). After removal of the histidine tag, crystals of space group I4$_1$22 that diffracted to 3 Å resolution at a synchrotron source (BM14 of the European Synchrotron Radiation Facility [ESRF], Grenoble, France) were obtained. The structure was determined using the multiple-wavelength anomalous dispersion (MAD) method.

Overall Structure

The sB7-1 monomer is a slender molecule, with dimensions of 23 × 30 × 90 Å^3, consisting of two anti-parallel β sandwich IgSF domains joined by a short linker region (Figure 1A). Thr-199 forms the last main chain hydrogen bond in the molecule and Ala-200 is well ordered but extends into solution. Between this residue and the probable first residue of the transmembrane domain (Leu-209), the native protein sequence consists of eight, mostly hydrophilic, residues likely to form an extended stalk linking the protein to the cell surface. Overall, the organization and dimensions of sB7-1 resemble those of the extracellular region of CD2 (Figure 1B), although there is a significant change in relative domain orientation (see below).

Immunoglobulin-like Domains

The amino-terminal domain (d1) of B7-1 has V-set topology (Williams and Barclay, 1988), with β strands forming DEB and AGFCC′C″ β sheets. Automated structure

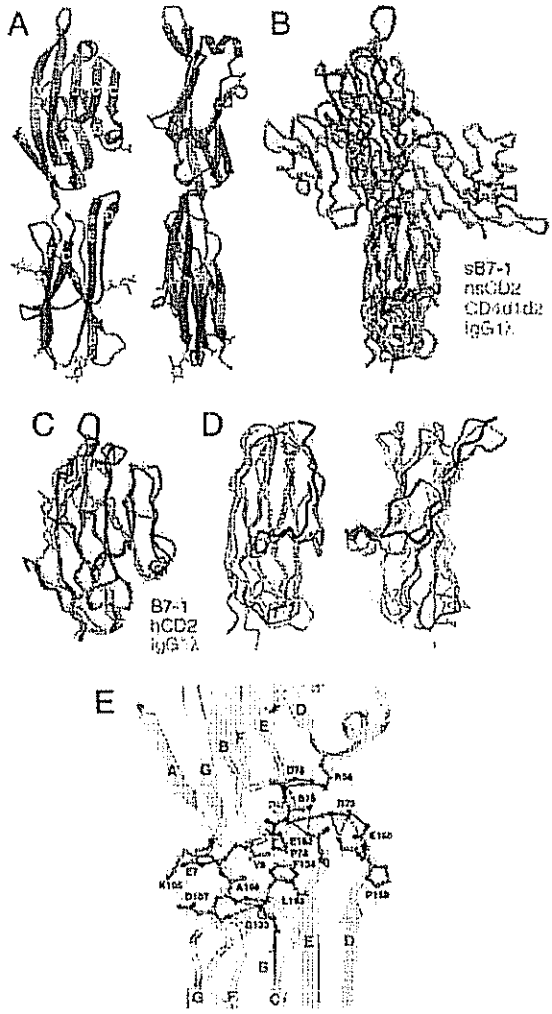


Figure 1. The Structure of the SeMet Form of sB7-1

(A) Two orthogonal views, shown in ribbon format, of the sB7-1 monomer. To indicate the course of the main chain, the color is varied from blue for residue 1 to red for residue 200. Asparagine residues that are part of glycosylation sequons are colored green and modeled with N-acetylglucosamine residues where electron density was sufficiently clear.

(B) Schematic α carbon representations of sB7-1, CD4d1d2 (1cdy), human sCD2 (1hnf), and IgG1 λ light chain (8fab) are shown superimposed on domain 2 of each molecule.

(C) Comparisons of the V-set IgSF domains of B7-1, human CD2 and IgG1 λ light chain.

(D) Two orthogonal views of domain 2 of B7-1 superimposed on the equivalent domains of IgG1 λ light chain and hCD2. The C′ or D strands are highlighted.

(E) The interdomain region of B7-1 with domain 1 and 2 colored red and green, respectively. The network of residues mediating interdomain contacts are shown in ball-and-stick representation.

comparisons (DALI; Holm and Sander, 1995) rank B7-1d1 as most similar to the membrane distal domains of CD2 (1hnf) and CD4 (1cdy), molecules involved in cell–cell adhesion. Superimpositions of the B7-1, CD2, and antibody (IgV_Lλ) V-set domains are shown in Figure 1C (rms differences between B7-1d1 and CD2d1 and the Ig domain are 1.1 Å and 1.3 Å for 89 and 81 equivalent Cα

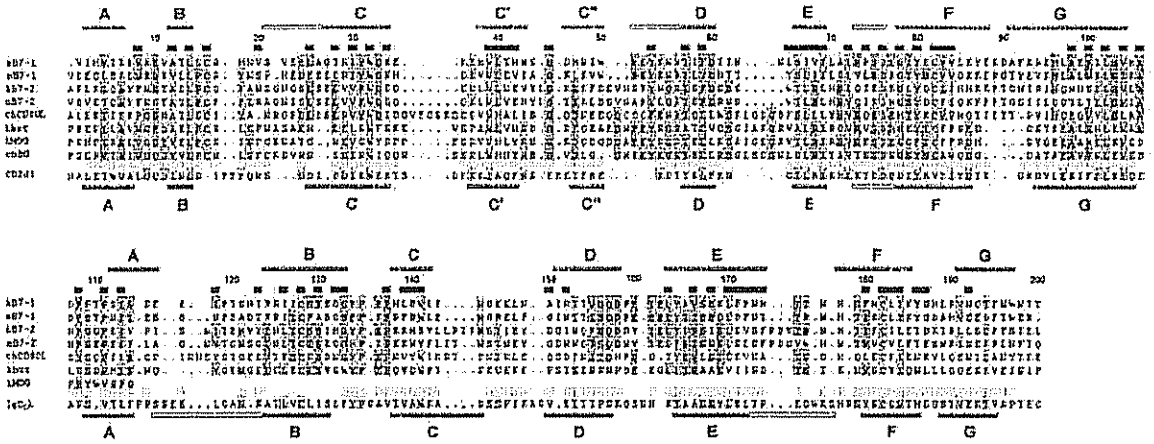


Figure 2. Alignment of B7 Subset and Human CD2 d1 and $IgC_L\lambda$ Sequences Based on the sB7-1, sCD2, and IgG1 λ Light Chain Crystal Structures

The B7 subset, initially defined by Linsley et al. (1994), is extended to include chicken CD80-like protein (chCD80L; TrEMBL accession number O42404). Alignments were done using CLUSTALW (Thompson et al., 1994) and then adjusted by eye. The structural alignments of B7-1 d1 and d2 with CD2 d1 and $IgC_L\lambda$, respectively, are based on the superpositions shown in Figure 1. Residues that are structurally equivalent in the superpositions are highlighted with yellow bars. Open and closed blue bars above the sequences mark α helices and β strands in the sB7-1 structure, respectively. Buried residues (i.e., those exposing less than 25 Å^2 of side chain surface area) are highlighted with red bars. Amino acids that exhibit a high degree of conservation in V and C1-set IgSF domains (Barclay et al., 1997) are colored blue, whereas those shaded orange are conserved only within the B7 subset sequences.

atoms, respectively). An important structural similarity shared by B7-1d1 and CD2d1, distinguishing these domains from antigen receptor V-set domains, is the lack of overall twist in the AGFCC′C″ sheet. This reflects the fact that B7-1d1 has its β bulges located immediately after the CC′ and FG turns at residues Met-38 and Arg-94, (equivalently positioned at residues Lys-43 and Asn-92 in human CD2d1; Bodian et al., 1994) rather than the C′ and G strand β bulges conserved in antigen receptor V-set domains.

In contrast to d1, the membrane proximal domain of B7-1 (d2) exhibits greater similarity to the constant domains of antigen receptors and the membrane proximal domains of MHC antigen-type structures than to the membrane proximal domain of cell–cell adhesion molecules. The d2 β sandwich is formed by DEBA and GFC β sheets typical of C1-set domains (Williams and Barclay, 1988). Thus, the six structures most similar to B7-1d2 selected by DALI all contain C1-set domains, and structural superposition of B7-1d2 with the constant domain of immunoglobulin λ light chain reveals greater similarity than the superposition of B7-1d2 with CD2d2 (rms differences of 1.4 Å and 1.5 Å for 80 and 64 equivalent residues, respectively; Figure 1D). The key structural feature is the organization of the strands at the "edge" of the domain: whereas beyond the C strand, CD2 has two short C′D strands extending the same β sheet, the B7-1 and the Fab C1-set domains have extended DE strands forming the first half of the second β sheet.

Interdomain Region

The interdomain "linkers" of B7-1 and human CD2 are identical in length (seven residues) and share remarkably similar main chain conformations, even though only Pro-111 and Ile-113 are conserved in both sequences (B7-1 sequence numbering). After superimposition of the membrane-proximal domains, the position of the membrane-distal (N-terminal) domain of sB7-1 differs from that of sCD2 by a rotation of 100° about the long axis of the molecule and a reduction of 20° in tilt relative to the same axis. The rotation occurs about Ala-106 of B7-1 (Glu-104 in CD2). The reduced tilt, and the much longer D and E strands of d2, result in the interdomain region of B7-1 burying a larger surface area (670 versus 590 Å^2) than is the case for CD2. This region consists of a buried, hydrophobic core formed by Val-8, Pro-74, Ala-106, Phe-134, and Leu-163. In addition, electrostatic contacts and main chain or side chain hydrogen bonds between Ser-75 and Glu-162, and between Arg-73 and both Pro-159 and Glu-160, appear to stabilize the extended, upright stature of the extracellular region of B7-1. The elaborate network of interactions supporting d1 is shown in Figure 1E.

The distinctive features of B7-1 define a new subset of the IgSF, into which sequence analysis groups B7-2, a chicken CD80-like protein (chCD80L), myelin/oligodendrocyte (hMOG) protein, the milk-fat globule membrane protein, butyrophilin (hbut), and the chicken MHC molecule, B-G antigen (chBG; Figure 2; Linsley et al., 1994; O'Regan et al., 1999). Although low, sequence identities indicate that these molecules have similar secondary and tertiary structures. The largest block of conserved residues that are not IgSF consensus residues lie in the D and E β strands and DE loop of domain 2. The conservation of this region, which is involved in the key interdomain electrostatic contacts, along with the conserved hydrophobicity of the interdomain core (residues 8, 106, 134, and 163), suggests that the frameworks of these molecules are likely to be similar.

Ligand Binding

Substantial losses (>90%) in ligand-binding activity occur when the solvent-exposed residues Arg-29, Tyr-31,

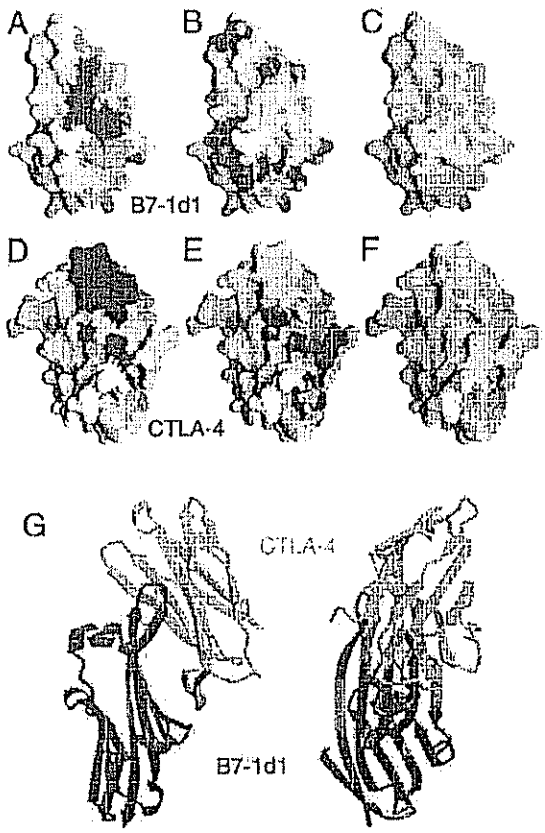


Figure 3. Properties of the Ligand Binding Faces of B7-1d1 and CTLA-4, and a Modeled Complex of these Molecules

In (A) (B7-1d1) and (D) (CTLA-4), the GRASP surfaces of residues whose mutation to alanine disrupts or has no effect on binding (Peach et al., 1995; Metzler et al., 1997) are colored magenta and cyan, respectively. In (B) and (E), the electrostatic potential calculated at neutral pH is shown projected onto the GRASP surfaces of each molecule; blue represents positive potential, white represents neutral, and red represents negative potential contoured at ± 8.5 kT. In (C) and (F), hydrophobicities calculated using GRID (P. Goodford, personal communication) are projected onto the GRASP surfaces of each molecule; yellow highlights regions of greatest hydrophobicity. The line of view in each panel is essentially perpendicular to the AGFCC'C'' ligand binding face of each molecule. In (G), the MYPPPY sequence of CTLA-4 implicated in B7-1 binding is highlighted as a darker blue loop in these two orthogonal views of the modeled complex.

Gln-33, Met-38, Ile-49, Trp-50, and Lys-86 of B7-1 are substituted with alanine (Figure 3A; Peach et al., 1995). With the exception of Lys-86, these residues form a contiguous, L-shaped cluster identifying the d1 AGFCC'C'' face as the ligand binding site of B7-1. Lys-86, which is not in the AGFCC'C'' face, may nevertheless form a salt bridge with Glu-24 in the BC loop that stabilizes the conformation of the FG loop. Not all of the residues surrounding this patch have been mutated, however, and it is likely that the full binding surface is substantially larger than this. Gln-33 is completely conserved in human and mouse B7-1 and B7-2, as are aromatic residues at position 31 and hydrophobic residues at position 38 (Figure 2). The conservation of these residues may explain the cross-reactivities of human and mouse B7-1 and B7-2 with human and mouse CD28 and CTLA-4.

It has been proposed that d2 residues form part of the B7-1 ligand-binding site (Peach et al., 1995). However, the relevant mutations (of DE loop residues Gln-157, Asp-158, and Glu-162) have much weaker effects on ligand binding (<50% inhibition) than mutations of the d1 AGFCC'C'' face and inspection of the structure suggests that such effects could result from changes in the presentation of d1 via alterations in the network of interactions at the domain interface (Figure 1E). Simple modeling also indicates that CTLA-4 cannot simultaneously bind both sets of residues. Furthermore, direct involvement of d2 would generate B7-1/ligand complexes spanning a much shorter intermembrane distance (~10 nm) than TCR/MHC complexes (~15 nm), creating a steric barrier to the CTLA-4/TCR interactions required for inhibitory signaling by CTLA-4 (Lee et al., 1999). For these reasons, we conclude that the d1 AGFCC'C'' face represents the principal ligand-binding surface of B7-1.

The AGFCC'C'' face of B7-1 is compositionally similar to other sites of protein–protein recognition and thus has substantially fewer charged and more hydrophobic residues than the equivalent face of CD2, which is also involved in low-affinity cell surface recognition (29% charged residues versus 45%–70% for CD2 [Bodian et al., 1994; Davis et al., 1998a]). Surface electrostatic potential is depicted in Figure 3B. Two hydrophobic residues essential for ligand binding, Met-38 and Trp-50, form a contiguous hydrophobic patch at the base of the AGFCC'C'' sheet of d1. In a complementary manner, the conserved MYPPPY sequence motif implicated in the binding of both CTLA-4 and CD28 to B7-1 and B7-2 (Figure 3D; Metzler et al., 1997), forms a hydrophobic patch centered on the FG loop of CTLA-4. The distribution of hydrophobicity on the surfaces of the AGFCC'C'' face of each molecule is shown in Figures 3C and 3F.

Manual docking of B7-1 d1 and CTLA-4, so that contact between the two hydrophobic patches and electrostatic complementarity are each maximized, and in a way that would permit interactions between adjacent cells, readily generates a feasible model for the complex of these two molecules (Figure 3G). The model is reminiscent of the antiparallel homophilic contacts observed in crystals of Protein 0 (Shapiro et al., 1996) and buries approximately 800 Å² of surface area per molecule, an area comparable to that buried in most other protein complexes (Janin and Chothia, 1990). The exaggerated twist of the AGFCC'C'' β sheet of CTLA-4 could allow extensive contact with the very long FG loop of B7-1, which appears to be a conserved feature of the B7-related sequences (Figure 2).

Molecular Association in the Crystal

A striking and unexpected feature of the sB7-1 crystal lattice is that it is dominated by a molecular contact at the 2-fold axis, which buries 610 Å² of surface area for each molecule. The lattice contact generates a compact dimer that, in overall shape and dimensions, is reminiscent of an antibody Fab′ molecule (Figure 4A). However, the dimer differs from a Fab′ insofar as the d1 interaction

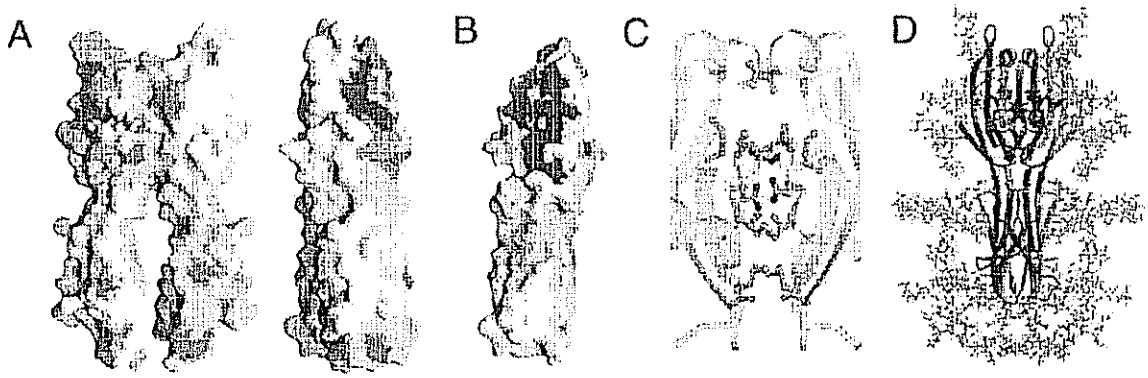


Figure 4 Structure of the sB7-1 Homodimer Observed in the Crystal Lattice

(A) Two orthogonal views of the GRASP surface of the homodimer showing the location of residues whose mutation to alanine disrupts (magenta) or has no effect (cyan) on binding. Putative N-glycosylation sites are colored green

(B) The GRASP surfaces of amino acids involved in forming the dimer are colored red. The view is identical to the right-hand panel in (A) but with the front copy of sB7-1 removed.

(C) Details of the residues at the dimer interface are shown in ball-and-stick format viewed as in the left-hand panel of (A).

(D) The homodimer is shown with either oligomannose-, bi-, or triantennary N-glycans modeled at each of the potential glycosylation sites

is mediated by a relatively flat surface formed by the B, C′, D, and E β strands rather than the AGFCC′C″ face, and there is no contact between d2 of each molecule (although such contacts might be possible in vivo and may only be precluded by this particular lattice). The interaction is mediated by the primarily hydrophobic residues (Val-11, Val-22, Gly-45, Met-47, Ile-58, Asp-60, Ile-61, Thr-62, and Leu-70) decorating the B, C′, D, and E β strands, leaving the AGFCC′C″ face free for ligand binding (Figures 4B and 4C). The molecules are inclined by 4° to the 2-fold axis, an arrangement consistent with the C-terminal stalks linking the molecules to the cell surface entering the membrane adjacently. The distribution of the glycosylation sites on the sB7-1 structure indicates that, even if all potential sites were to be fully utilized, the dimer interface would be free of N-linked glycans (Figures 4A and 4D).

Dimerization of sB7-1 in Solution

Analytical ultracentrifugation at a range of concentrations and at three temperatures (Figures 5A and 5B; see Experimental Procedures) indicates that sB7-1 undergoes dimerization in solution with a K_d in the range of 20–50 μM. At higher concentrations, aggregation also occurred (data not shown). These effects are reversible, and sedimentation velocity boundary analysis (Stafford, 1992) of samples in a concentration range where both monomer and dimer were present was unable to differentiate between the species, indicating that monomer and dimer are in rapid exchange with a rate constant of dissociation greater than 10^{-2} s^{-1} (Cann, 1986). The temperature dependence of the K_d is consistent with the largely hydrophobic nature of the contact seen in the crystal lattice.

Discussion

The relationship of the structure of the extracellular region of B7-1 to its function is illuminated by comparison with CD2. A key structural difference between B7-1 and CD2 lies in d2 of each molecule. In B7-1 this domain is topologically similar to C1-set domains, which have

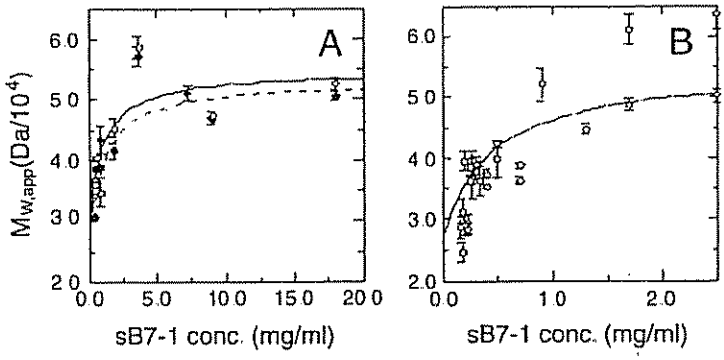


Figure 5 Analytical Ultracentrifugation of sB7-1

Apparent whole-cell weight-average molecular weight ($M_{w,app}$) of sB7-1 as a function of sample loading concentration at 4°C (closed circles) and 20°C (open circles) (A) and at 37°C (open circles) (B). The 4°C (dashed line, [A]), 20°C (solid line, [A]), and 37°C (solid line, [B]) data have been fitted to equation 2 to obtain apparent dissociation constants. The trends in $M_{w,app}$ indicate that sB7-1 is undergoing self-association and is in dynamic equilibrium between a monomeric form ($M_{w,app}$ ~ 27 kDa) and a dimeric form ($M_{w,app}$ ~54 kDa). The parameters given by the fits to the data for sB7-1 are a monomer mass (M_1) of 26609 ± 2206 Da, with a dissociation constant K_d of 44 μM at 4°C; an M_1 of 27384 ± 1942 Da, K_d of 33 μM at 20°C; and an M_1 of 27478 ± 3176 Da, with a dissociation constant K_d of 17 μM at 37°C.

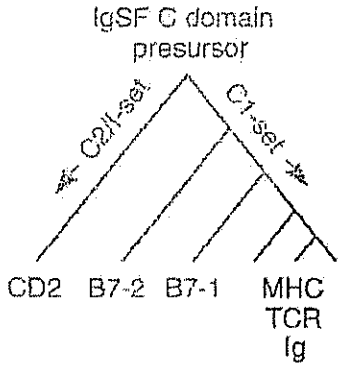


Figure 6 Evolutionary Relationships of the IgSF Constant-like Domains

The parts of the lineage colored blue are proposed to have generated cell adhesion and cell–cell recognition molecules, whereas the red section produced components of the adaptive immune response. CD2 is used to represent the C2/I-set.

previously only been observed in the structures of antigen receptors and MHC antigens; in contrast, CD2d2 belongs to the C2-set. The ALIGN program (Dayhoff et al., 1983) gives significantly higher scores for comparisons of human and mouse B7-1d2 sequences with representative C1-set sequences (Barclay et al., 1997) than for C2-set sequences (5.4 ± 0.56 versus 2.79 ± 1.99, respectively). Thus, both topology and sequence place d2 of B7-1 within the C1-set. However, the ALIGN scores for B7-1d2 comparisons with other C1-set sequences are significantly lower than for comparisons within the classic C1-set (8.5 ± 2.7). This implies that the appearance of B7-1-like molecules may have predated the evolution of distinct antigen receptors and MHC antigens. B7-1 and B7-2, while clearly related, share very limited sequence similarity, and human and mouse B7-2d2 give equally poor matches with both C1- and C2-set sequences (2.3 ± 0.9 and 2.2 ± 1.1), suggesting that B7-2 might be even more primitive. Taken with the observation that the adhesion domains of B7-1 and CD2 are remarkably similar, these data suggest a set of evolutionary relationships in which the earliest members of the C1-set are adhesion molecules, and antigen receptors essential for adaptive immune responses (characterized by GFCC'C'' β sheet mediated V-set heterodimerization [Springer, 1991]) appear late in the evolution of the IgSF (Figure 6). Similarity between domain 2 of B7-1 and the C1-set domain of β2-microglobulin was predicted by Bajorath et al. (1994), and the genetic linkage of B7-related molecules to the MHC has been noted previously (Henry et al., 1997).

Although sB7-1 and sCD2 have similar overall dimensions, the reduced tilt of domain 1 relative to domain 2 positions the ligand binding AGFCC'C'' face of B7-1 normal to the long axis of the molecule rather than, as in CD2, parallel with it (Jones et al., 1992; Bodian et al., 1994). Such differences may be related to the sequence of expression of these genes. Maximum exposure of the ligand binding face at the "top" of the molecule may be crucial for establishing the initial contact zone between T cells and antigen-presenting cells by CD2 (van der Merwe et al., 1995; Davis and van der Merwe, 1996; Dustin et al., 1998). B7-1 appears after formation of the contact zone, however, when the interacting cell surfaces are already optimally aligned for interactions involving molecules the size of B7-1, the T cell receptor, and their respective ligands. An important consequence of the essentially parallel alignment of d1 and d2 of B7-1 is that it exposes the non-ligand-binding DEB face of d1, allowing the formation of parallel, compact homodimers. The formation of equivalent dimers by CD2 is precluded by the 42° tilt in the position of d1 relative to the long axis of the molecule (Jones et al., 1992; Bodian et al., 1994).

Functionally distinct interactions are suggested by the presence of radically different molecular contacts in the crystal lattices of sB7-1 and sCD2. sCD2 packs head-to-head, an arrangement which was predicted (Jones et al., 1992) and subsequently shown (Wang et al., 1999) to mimic natural receptor-ligand interactions. In contrast, the sB7-1 crystal lattice is dominated by a side–side molecular contact that generates a potentially bivalent homodimer. Model studies indicate that cell surface proteins with solution affinities in the range of 15–75 μM interact spontaneously at membrane interfaces (Dustin et al., 1996; 1997). The K_d of 20–50 μM for dimerization and rapid monomer–dimer exchange we have observed

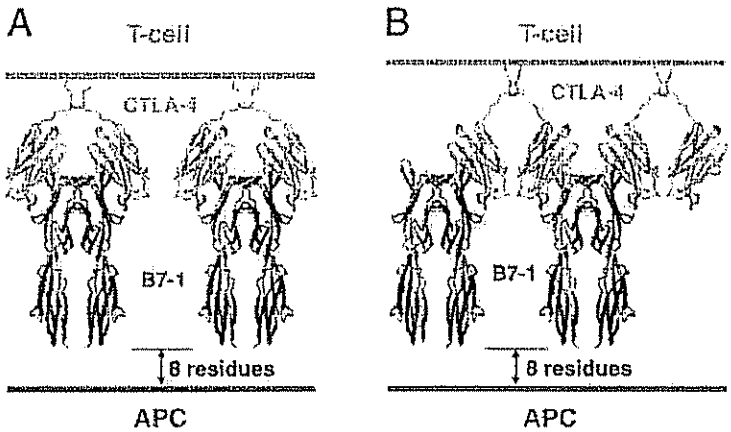


Figure 7. Potential Molecular Complexes Formed by the B7-1 and CTLA-4 Homodimers at the Cell Surface

The B7-1 homodimer shown is identical to that observed in the crystal lattice. The CTLA-4 homodimer is based on the solution structure of the monomer (Metzler et al., 1997), with the sequence connecting β strand G to the intermolecular disulphide at Cys-123 modeled in extended conformation. The ligand-binding domains of B7-1 and CTLA-4 are docked as described in the text, allowing the formation of two potential types of complexes: paired homodimers (A) and complexes in which separate sB7-1 homodimers are bridged by adjacent CTLA-4 dimers (B).

Table 1. Data Collection and Refinement Statistics

Data Processing				
Wavelength (Å)	0.8855	0.9793	0.9796	all
Observation	34,375	34,531	36,114	105,456
Unique*	9,341	9,349	9,436	5,409
Redundancy	3.7	3.7	3.8	19.5
$<I/\sigma(I)>$	12 (3)	10 (2)	11 (2)	24 (5)
R_{merge} (%)	9.2 (42)	9.3 (43)	9.2 (42)	11.4 (48)
Resolution (Å)		20–3.0 (3.1–3.0)		
Completeness (%)	98 (93)	99 (96)	99 (93)	100 (99)

Refinement	
Data range (Å)	20–3.0 (3.1–3.0)
Reflections (F>0)	5,204 (283)
Completeness (%)	96.5 (88.9)
Reflections in R_{free} set	289 (21)
Nonhydrogen atoms (protein/sugar)	1,604/42
Rms Δ bond lengths (Å)	0.008
Rms Δ bond angles (°)	1.4
Rms Δ B factors for bonded atoms (Å²) (main/side)	1.3/1.9
Mean B factors (Å²) (main/side/sugar)	41.4/42.8/49.0
Mean main chain B factors (Å²) (domain 1/domain 2)	45.2/37.2
R_{free} (%)	28.2 (35.4)
R_{cryst} (%)	23.7 (34.1)

* For data sets collected at individual wavelengths. Bijvoet pairs were not merged. However, the Bijvoet pairs were merged in the data set generated by merging the data collected at all wavelengths.
Values in parentheses correspond to the highest resolution shell (3.1–3.0 Å).
$R_{merge} = \Sigma|I - <I>|/\Sigma<I>$
$R_{cryst} = \Sigma||F_{obs}| - |F_{calc}||/\Sigma|F_{obs}|$
R_{free} = as for R_{cryst} but calculated for a test set comprising reflections not used in the refinement.
Root mean squared deviations (rms Δ) in bond length and angles are given from ideal values.

suggests that B7-1 may exist at the cell surface in a dynamic equilibrium dominated by a homodimer similar to that observed in the crystal. Since CTLA-4 exists as a disulfide-bonded homodimer, the existence of B7-1 dimers would allow two types of multivalent associations to form at the cell–cell interface, one involving paired homodimers (Figure 7A), the alternative involving a dimer of B7-1 bridging adjacent CTLA-4 dimers (Figure 7B). Simple modeling studies suggest that the second type of interaction might be sterically favored.

CTLA-4 is not expressed on resting T cells, and the level of CTLA-4 expression at the cell surface is kept very low, even on activated cells (Linsley et al., 1992a). CTLA-4 is also stored in intracellular vesicles (Leung et al., 1995) whose release is directed at the contact zone between activated T cells and antigen-presenting cells (Linsley et al., 1996). This suggests that its release into and sequestration within the central supramolecular activation cluster (cSMAC) of the immunological synapse (Monks et al., 1998; Grakoui et al., 1999) is key to the inhibitory function of CTLA-4. The solution affinity of B7-1 for CTLA-4 (~0.2–0.4 μM) is among the highest described for interacting cell surface molecules (reviewed in Davis et al., 1998b), at least 10-fold higher than the affinity of B7-1/CD28 interactions (~4 μM; van der Merwe et al., 1997) and 40- to 100-fold higher than that of B7-2/CD28 interactions (~15 μM; A. V. C. et al., unpublished data). The avidity model proposed in Figure 7B would provide a mechanism for further stabilizing the interaction of B7-1 with CTLA-4 within the cSMAC. While it is clear that B7-1/CD28 interactions may generate competing costimulatory signals, the foregoing structural considerations, along with the timing of B7-1 and CTLA-4 expression, suggest that a key function of B7-1 is to generate particularly stable signaling complexes with CTLA-4 late in immune responses, increasing the likelihood of inhibitory signaling by CTLA-4 and facilitating the termination of T cell activation.

Experimental Procedures

Protein Expression and Crystallization

The expression of a construct encoding a histidine-tagged form of sB7-1, consisting of residues 1–201 of the native protein and bearing a deleted C-terminal glycosylation site (Asn-198), in Lec3.2.8.1 cells in the presence of 0.5 mM N-butyl deoxynojirimycin is described by Butters et al. (1999). SeMet labeling was done according to the method of May et al. (1997). After removal of the histidine tag with carboxypeptidase A (van der Merwe et al., 1997), data collection–quality wild-type and SeMet sB7-1 crystals grew readily in sitting drops containing 2 μl of protein (at an optical density of 20–30 in 10 mM HEPES, 140 mM NaCl, 0.05% NaN_3 [pH 7.4]) and 2 μl of reservoir solution (typically a 10%–90% v/v dilution of a stock solution containing 28% PEG 400, 0.1M Na HEPES (pH 7.5), 0.2M $CaCl_2$).

Structure Determination

The crystals belong to space group I4,22 (cell dimensions a = b = 57.3 Å, c = 298.9 Å, consistent with a single molecule per asymmetric unit). For data collection at 100 K, crystals were briefly transferred to mother liquor containing 10% v/v glycerol. Molecular replacement and multiple isomorphous replacement phasing attempts failed (high levels of nonisomorphism were apparent between native and heavy atom data sets). Diffraction data for MAD-based phase determination were collected from one cryo-cooled SeMet sB7-1 crystal at station BM14 of the ESRF. The Se absorption edge was located by a fluorescence scan, and consecutive data sets were collected at three wavelengths (λ = 0.8855 Å, 0.97930 Å, and 0.97955 Å, the latter wavelengths being at the white line and inflection point) using

the 180 mm scan mode of a 345 mm diameter MAR-Research (Hamburg, Germany) image plate detector. The diffraction data were processed and scaled with the HKL program suite (Otwinowski and Minor, 1997; statistics reported in Table 1). The expected six Se atom positions were determined, refined, and phases calculated to 3.0 Å resolution, using the program SOLVE (Terwilliger and Berendzen, 1997). An initial electron density map based on these phases was improved with programs DM and SOLOMON (CCP4, 1994) to yield a high quality electron density map. The structure was built using program O (Jones et al., 1991). The entire course of the main chain was apparent; however, only half the true side chains were built, with the remainder initially modeled as alanines.

Refinement with CNS (Brunger et al., 1998) used a set of F_{obs} constructed by merging the diffraction data (including Bijvoet pairs) from all three MAD wavelengths. After some refinement and manual rebuilding, the entire sB7-1 sequence was fitted and clear electron density allowed the unambiguous positioning of three N-linked N-acetylglucosamine residues. Further refinement of the atomic positions and tightly restrained individual isotropic B-factors resulted in a final crystallographic R_{factor} and R_{free} of 23.7% and 28.2%, respectively. In the final model, 80.4% of residues fall in the most favored regions of the Ramachandran plot and no nonglycine residues fall in disallowed regions (Laskowski et al., 1993). Refinement and model statistics are reported in Table 1.

Structural superpositions used program SHP (Stuart et al., 1979). Figures 1–3, 6, 7, and 9 were produced using programs BOBSCRIPT (Esnouf, 1997) and Raster3D (Merritt and Murphy, 1994). Electrostatic analysis and surface display for Figures 5 and 7 used the program GRASP (Nicholls et al., 1991).

Analytical Ultracentrifugation Methods

Analytical ultracentrifugation used a Beckman Instruments Optima XL-A equipped with scanning absorbance optics utilizing wavelengths of 225 nm, 230 nm, 254 nm, 280 nm, 300 nm, 310 nm, and 320 nm, depending on the protein concentrations present (Tuma et al., 1996). Thermodynamic equilibrium was taken to have been reached when distribution scans acquired 3 hr apart were coincident. The experiments were performed at a rotor speed of 10,000 rpm, and the sample was pelleted from solution at 40,000 rpm following the attainment of equilibrium to allow the baseline absorbance to be measured. The data were fitted with the equation

$$A(r) = A(r_f)\exp\left[\frac{(1 - \bar{\nu}\rho)\omega^2}{2RT}(r^2 - r_f^2)\right] + E \qquad (1)$$

where $A(r)$ is the absorbance at radius r (in cm). $A(r_f)$ is the absorbance at reference radius r_f. $\bar{\nu}$ is the partial specific volume (in ml/g). ρ is the solvent density (in g/ml). ω is the angular velocity of the centrifuge rotor (in rad/s). R is the gas constant. T the absolute temperature, and E the baseline offset. By comparing the apparent mass of the glycosylated sB7-1 molecules determined using SDS-PAGE with the known mass of the polypeptide alone, the percent by weight sugar was estimated. The weighted average $\bar{\nu}$ was calculated as 0.687 ml/g using known values for the partial volumes of amino acids and sugars (Perkins, 1986). The whole-cell weight-average apparent molecular weights obtained through fitting Equation 1 to the equilibrium distributions were plotted against the concentration at the midpoint of the distribution (Laue, 1992) to obtain diagnostics of the solution behavior of the samples. These curves were fitted with the equation

$$M_{w,app} = \frac{(n - 1)M_1 c}{K_d + c} + M_1 \qquad (2)$$

where $M_{w,app}$ is the apparent whole-cell weight-average molecular weight (in Da) obtained from fitting equation 1. n is the association state of the complex formed by the protein, M_1 is the monomer mass of the protein, c is the protein concentration, and K_d is the dissociation constant of the protein complex (in units of c).

Acknowledgments

The authors thank P. Sorensen, V. Avery, P. A. van der Merwe, and W. F. Stafford for advice and comments on the manuscript and B. J. Classon for assistance with the sequence comparisons. This work was supported by the Arthritis Research Campaign, the Biotechnology and Biological Sciences Research Council, the Engineering and Physical Sciences Research Council, the Medical Research Council, the Royal Society and the Wellcome Trust. S. I. and D. I. S. are members of the Tsukuba Advanced Research Alliance project of Tsukuba University, Tsukuba, Japan. The analytical ultracentrifugation experiments were performed in the AUC facility established by the BBSRC and the Wellcome Trust in the Glycobiology Institute of the University of Oxford. The facility is managed by Dr. Russell Wallis.

Received November 2, 1999; revised December 16, 1999

References

Aruffo, A., and Seed, B. (1987). Molecular cloning of a CD28 cDNA by a high-efficiency COS cell expression system. Proc. Natl. Acad. Sci. USA *84*, 8573–8577.

Azuma, M., Ito, D., Yagita, H., Okumura, K., Phillips, J.H., Lanier, L.L., and Somoza, C. (1993). B70 antigen is a second ligand for CTLA-4 and CD28. Nature *366*, 76–79.

Bajorath, J., Peach, R.J., and Linsley, P.S. (1994). Immunoglobulin fold characteristics of B7-1 (CD80) and B7-2 (CD86). Protein Sci. *3*, 2148–2150.

Barclay, A.N., Brown, M.H., Law, S.K.A., McKnight, A.J., Tomlinson, M.G., and van der Merwe, P.A. (1997). The Leukocyte Antigen Facts-book (London: Academic Press).

Bodian, D.L., Jones, E.Y., Harlos, K., Stuart, D.I., and Davis, S.J. (1994). Crystal structure of the extracellular region of the human cell adhesion molecule CD2 at 2.5 Å resolution. Structure *15*, 755–766.

Borriello, F., Sethna, M.P., Boyd, S.D., Schweitzer, A.N., Tivol, E.A., Jacoby, D., Strom, T.B., Simpson, E.M., Freeman, G.J., and Sharpe, A.H. (1997). B7-1 and B7-2 have overlapping, critical roles in immunoglobulin class switching and germinal center formation. Immunity *6*, 303–313.

Brunet, J.F., Denizot, F., Luciani, M.F., Roux-Dosseto, M., Suzan, M., Mattei, M.G., and Golstein, P. (1987). A new member of the immunoglobulin superfamily—CTLA-4. Nature *328*, 267–270.

Brunger, A.T., Adams, P.D., Clore, G.M., DeLano, W.L., Gros, P., Grosse-Kunstleve, R.W., Jiang, J.S., Kuszewski, J., Nilges, M., Pannu, N.S., et al. (1998). Crystallography and NMR system: a new software suite for macromolecular structure determination. Acta Crystallogr. D Biol. Crystallogr. *54*, 905–921.

Butters, T.D., Sparks, L.M., Harlos, K., Ikemizu, S., Stuart, D.I., Jones, E.Y., and Davis, S.J. (1999). Additive effects of *N*-butyldeoxynojirimycin and the Lec3.2.8.1 mutant phenotype on N-glycan processing in chinese hamster ovary cells: application to glycoprotein crystallisation. Proteins *8*, 1707–1712.

Cann, J.R. (1986). Effects of microheterogeneity on sedimentation patterns of interacting proteins and the sedimentation behavior of systems involving two ligands. Methods Enzymol. *130*, 19–35.

CCP4 (1994). Collaborative Computational Project, Number 4. The CCP4 suite: programs for protein crystallography. Acta Cryst. D *50*, 760–763.

Chen, L., Ashe, S., Brady, W.A., Hellstrom, I., Hellstrom, K.E., Ledbetter, J.A., McGowan, P., and Linsley, P.S. (1992). Costimulation of antitumor immunity by the B7 counterreceptor for the T lymphocyte molecules CD28 and CTLA-4. Cell *71*, 1093–1102.

Davis, S.J., and van der Merwe, P.A. (1996). The structure and ligand interactions of CD2: implications for T-cell function. Immunol. Today *17*, 177–187.

Davis, S.J., Davies, E.A., Tucknott, M.G., Jones, E.Y., and van der Merwe, P.A. (1998a). The role of charged residues mediating low affinity protein-protein recognition at the cell surface by CD2. Proc. Natl. Acad. Sci. USA *95*, 5490–5494.

Davis, S.J., Ikemizu, S., Wild, M.K., and van der Merwe, P.A. (1998b). CD2 and the nature of protein interactions mediating cell-cell recognition. Immunol. Rev. *163*, 217–236.

Dayhoff, M.O., Barker, W.C., and Hunt, L.T. (1983). Establishing homologies in protein sequences. Methods Enzymol. *91*, 524–545.

Dustin, M.L., Ferguson, L.M., Chan, P.Y., Springer, T.A. and Golan, D.E. (1996). Visualization of CD2 interaction with LFA-3 and determination of the two-dimensional dissociation constant for adhesion receptors in a contact area. J. Cell. Biol. *132*, 465–474.

Dustin, M.L., Golan, D.E., Zhu, D.M., Miller, J.M., Meier, W., Davies, E.A., and van der Merwe, P.A. (1997). Low affinity interaction of human or rat T cell adhesion molecule CD2 with its ligand aligns adhering membranes to achieve high physiological affinity. J. Biol. Chem. *272*, 30889–30898.

Dustin, M.L., Olszowy, M.W., Holdorf, A.D., Li, J., Bromley, S., Desai, N., Widder, P., Rosenberger, F., van der Merwe, P.A., Allen, P.M., and Shaw, A.S. (1998). A novel adaptor protein orchestrates receptor patterning and cytoskeletal polarity in T-cell contacts. Cell *94*, 667–677.

Esnouf, R.M. (1997). An extensively modified version of MolScript that includes greatly enhanced coloring capabilities. J. Mol. Graph. Model. *15*, 132–134, 112–113.

Finck, B.K., Linsley, P.S., and Wofsy, D. (1994). Treatment of murine lupus with CTLA4Ig. Science *265*, 1225–1227.

Freeman, G.J., Freedman, A.S., Segil, J.M., Lee, G., Whitman, J.F., and Nadler, L.M. (1989). B7, a new member of the Ig superfamily with unique expression on activated and neoplastic B cells. J. Immunol. *143*, 2714–2722.

Freeman, G.J., Gribben, J.G., Boussiotis, V.A., Ng, J.W., Restivo, V.A., Jr., Lombard, L.A., Gray, G.S., and Nadler, L.M. (1993a). Cloning of B7-2: a CTLA-4 counter-receptor that costimulates human T cell proliferation. Science *262*, 909–911.

Freeman, G.J., Borriello, F., Hodes, R.J., Reiser, H., Hathcock, K.S., Laszlo, G., McKnight, A.J., Kim, J., Du, L., Lombard, D.B., et al. (1993b). Uncovering of functional alternative CTLA-4 counter-receptor in B7-deficient mice. Science *262*, 907–909.

Freeman, G.J., Boussiotis, V.A., Anumanthan, A., Bernstein, G.M., Ke, X.Y., Rennert, P.D., Gray, G.S., Gribben, J.G., and Nadler, L.M. (1995). B7-1 and B7-2 do not deliver identical costimulatory signals, since B7-2 but not B7-1 preferentially costimulates the initial production of IL-4. Immunity *2*, 523–532.

Grakoui, A., Bromley, S.K., Sumen, C., Davis, M.M., Shaw, A.S., Allen, P.M., and Dustin, M.L. (1999). The immunological synapse: a molecular machine controlling T cell activation. Science *285*, 221–227.

Greenfield, E.A., Nguyen, K.A., and Kuchroo, V.K. (1998). CD28/B7 costimulation: a review. Crit. Rev. Immunol. *18*, 389–418.

Guinan, E.C., Boussiotis, V.A., Neuberg, D., Brennan, L.L., Hirano, N., Nadler, L.M., and Gribben, J.G. (1999). Transplantation of anergic histoincompatible bone marrow allografts. N. Engl. J. Med. *340*, 1704–1714.

Harding, F.A., McArthur, J.G., Gross, J.A., Raulet, D.H., and Allison, J.P. (1992). CD28-mediated signaling co-stimulates murine T cells and prevents induction of anergy in T-cell clones. Nature *356*, 607–609.

Henry, J., Ribouchon, M., Depetris, D., Mattei, M., Offer, C., Tazi-Ahnini, R., and Pontarotti, P. (1997). Cloning, structural analysis, and mapping of the B30 and B7 multigenic families to the major histocompatibility complex (MHC) and other chromosomal regions. Immunogenetics *46*, 383–395.

Holm, L., and Sander, C. (1995). Dali: a network tool for protein structure comparison. Trends Biochem. Sci. *20*, 478–480.

Hutloff, A., Dittrich, A.M., Beier, K.C., Eljaschewitsch, B., Kraft, R., Anagnostopoulos, I., and Kroczek, R.A. (1999). ICOS is an inducible T-cell co-stimulator structurally and functionally related to CD28. Nature *397*, 263–266.

Janin, J., and Chothia, C. (1990). The structure of protein-protein recognition sites. J. Biol. Chem. *265*, 16027–16030.

Jones, E.Y., Davis, S.J., Williams, A.F., Harlos, K., and Stuart, D.I. (1992). Crystal structure at 2.8 Å resolution of a soluble form of the cell adhesion molecule CD2. Nature *360*, 232–239.

Jones, T.A., Zou, J.Y., Cowan, S.W., and Kjeldgaard, M. (1991). Improved methods for finding protein models in electron density maps and the location of errors in these models. Acta Crystallogr. A *47*, 110–119.

Kuchroo, V.K., Das, M.P., Brown, J.A., Ranger, A.M., Zamvil, S.S., Sobel, R.A., Weiner, H.L., Nabavi, N., and Glimcher, L.H. (1995). B7-1 and B7-2 costimulatory molecules activate differentially the Th1/Th2 developmental pathways: application to autoimmune disease therapy. Cell *80*, 707–718.

Larsen, C.P., Elwood, E.T., Alexander, D.Z., Ritchie, S.C., Hendrix, R., Tucker-Burden, C., Cho, H.R., Aruffo, A., Hollenbaugh, D., Linsley, P.S., et al. (1996). Long-term acceptance of skin and cardiac allografts after blocking CD40 and CD28 pathways. Nature *381*, 434–438.

Laskowski, R.A., MacArthur, M.W., Moss, D.S., and Thornton, J.M. (1993). PROCHECK: a program to check the stereochemical quality of protein structures. J. Appl. Cryst. *26*, 283–291.

Laue, T.M. (1992). Technical Information DS-835 (Palo Alto, CA: Spinco Business Unit).

Leach, D.R., Krummel, M.F., and Allison, J.P. (1996). Enhancement of antitumor immunity by CTLA-4 blockade. Science *271*, 1734–1736.

Lee, K.M., Chuang, E., Griffin, M., Khattri, R., Hong, D.K., Zhang, W., Straus, D., Samelson, L.E., Thompson, C.B., and Bluestone, J.A. (1999). Molecular basis of T cell inactivation by CTLA-4. Science *282*, 2263–2266.

Lenschow, D.J., Walunas, T.L., and Bluestone, J.A. (1996). CD28/B7 system of T cell costimulation. Annu. Rev. Immunol. *14*, 233–258.

Leung, H.T., Bradshaw, J., Cleaveland, J.S., and Linsley, P.S. (1995). Cytotoxic T lymphocyte-associated molecule-4, a high-avidity receptor for CD80 and CD86, contains an intracellular localization motif in its cytoplasmic tail. J. Biol. Chem. *270*, 25107–25114.

Linsley, P.S., Greene, J.L., Tan, P., Bradshaw, J., Ledbetter, J.A., Anasetti, C., and Damle, N.K. (1992a). Coexpression and functional cooperation of CTLA-4 and CD28 on activated T lymphocytes. J. Exp. Med. *176*, 1595–1604.

Linsley, P.S., Wallace, P.M., Johnson, J., Gibson, M.G., Greene, J.L., Ledbetter, J.A., Singh, C., and Tepper, M.A. (1992b). Immunosuppression in vivo by a soluble form of the CTLA-4 T cell activation molecule. Science *257*, 792–795.

Linsley, P.S., Peach, R., Gladstone, P., and Bajorath, J. (1994). Extending the B7 (CD80) gene family. Protein Sci. *3*, 1341–1343.

Linsley, P.S., Bradshaw, J., Greene, J., Peach, R., Bennett, K.L., and Mittler, R.S. (1996). Intracellular trafficking of CTLA-4 and focal localization towards sites of TCR engagement. Immunity *4*, 535–543.

Mandelbrot, D.A., McAdam, A.J., and Sharpe, A.H. (1999). B7-1 or B7-2 is required to produce the lymphoproliferative phenotype in mice lacking cytotoxic T lymphocyte-associated antigen 4 (CTLA-4). J. Exp. Med. *189*, 435–440.

Marengere, L.E., Waterhouse, P., Duncan, G.S., Mittrucker, H.W., Feng, G.S., and Mak, T.W. (1996). Regulation of T cell receptor signaling by tyrosine phosphatase SYP association with CTLA-4. Science *272*, 1170–1173.

Martin, P.J., Ledbetter, J.A., Morishita, Y., June, C.H., Beatty, P.G., and Hansen, J.A. (1986). A 44 kilodalton cell surface homodimer regulates interleukin 2 production by activated human T lymphocytes. J. Immunol. *136*, 3282–3287.

May, A.P., Robinson, R.C., Aplin, R.T., Bradfield, P., Crocker, P.R., and Jones, E.Y. (1997). Expression, crystallization, and preliminary X-ray analysis of a sialicacid-binding fragment of sialoadhesin in the presence and absence of ligand. Protein Sci. *6*, 717–721.

McAdam, A.J., Schweitzer, A.N., and Sharpe, A.H. (1998). The role of B7 co-stimulation in activation and differentiation of CD4+ and CD8+ T cells. Immunol. Rev. *165*, 231–247.

Merritt, E.A., and Murphy, M.E.P. (1994). Raster3D version 2.0: a program for photorealistic molecular graphics. Acta Cryst. D *50*, 869–873.

Metzler, W.J., Bajorath, J., Fenderson, W., Shaw, S.Y., Constantine, K.L., Naemura, J., Leytze, G., Peach, R.J., Lavoie, T.B., Mueller, L., and Linsley, P.S. (1997). Solution structure of human CTLA-4 and delineation of a CD80/CD86 binding site conserved in CD28. Nat. Struct. Biol. *4*, 527–531.

Monks, C.R., Freiberg, B.A., Kupfer, H., Sciaky, N., and Kupfer, A.

(1998). Three-dimensional segregation of supramolecular activation clusters in T cells. Nature *395*, 82–86.

Nicholls, A., Sharp, K.A., and Honig, B. (1991). Protein folding and association: insights from the interfacial and thermodynamic properties of hydrocarbons. Proteins *11*, 281–296.

Olsson, C., Riebeck, K., Dohlsten, M., and Michaelsson, E. (1999). CTLA-4 ligation suppresses CD28-induced NF-kappaB and AP-1 activity in mouse T cell blasts. J. Biol. Chem. *274*, 14400–14405.

O'Regan, M.N., Parsons, K.R., Tregaskes, C.A., and Young, J.R. (1999). A chicken homologue of the co-stimulating molecule CD80 which binds to mammalian CTLA-4. Immunogenetics *1*, 68–71.

Otwinowski, Z., and Minor, W. (1997). Processing of X-ray diffraction data collected in oscillation mode. Methods Enzymol. *276*, 307–326.

Peach, R.J., Bajorath, J., Naemura, J., Leytze, G., Greene, J., Aruffo, A., and Linsley, P.S. (1995). Both extracellular immunoglobin-like domains of CD80 contain residues critical for binding T cell surface receptors CTLA-4 and CD28. J. Biol. Chem. *8*, 21181–21187.

Perkins, S.J. (1986). Protein volumes and hydration effects. The calculations of partial specific volumes, neutron scattering matchpoints and 280-nm absorption coefficients for proteins and glycoproteins from amino acid sequences. Eur. J. Biochem. *157*, 169–180.

Schweitzer, A.N., Borriello, F., Wong, R.C., Abbas, A.K., and Sharpe, A.H. (1997). Role of costimulators in T cell differentiation: studies using antigen-presenting cells lacking expression of CD80 or CD86. J. Immunol. *158*, 2713–2722.

Shapiro, L., Doyle, J.P., Hensley, P., Colman, D.R., and Hendrickson, W.A. (1996). Crystal structure of the extracellular domain from P0, the major structural protein of peripheral nerve myelin. Neuron *17*, 435–449.

Slavik, J.M., Hutchcroft, J.E., and Bierer, B.E. (1999). CD80 and CD86 are not equivalent in their ability to induce the tyrosine phosphorylation of CD28. J. Biol. Chem. *274*, 3116–3124.

Springer, T.A. (1991). Cell adhesion. A birth certificate for CD2. Nature *353*, 704–705.

Stafford, W.F., III (1992). Boundary analysis in sedimentation transport experiments: a procedure for obtaining sedimentation coefficient distributions using the time derivative of the concentration profile. Anal. Biochem. *203*, 295–301.

Stuart, D.I., Levine, M., Muirhead, H., and Stammers, D.K. (1979). Crystal structure of cat muscle pyruvate kinase at a resolution of 2.6 Å. J. Mol. Biol. *134*, 109–142.

Terwilliger, T.C., and Berendzen, J. (1997). Bayesian MAD phasing. Acta Cryst. D *53*, 571–579.

Thompson, J.D., Higgins, D.G., and Gibson, T.J. (1994). CLUSTAL W: improving the sensitivity of progressive multiple sequence alignment through sequence weighting, position-specific gap penalties and weight matrix choice. Nucleic Acids Res. *22*, 4673–4680.

Townsend, S.E., and Allison, J.P. (1993). Tumor rejection after direct costimulation of CD8+ T cells by B7-transfected melanoma cells. Science *259*, 368–370.

Tuma, R., Bamford, J.H., Bamford, D.H., Russell, M.P., and Thomas, G.J., Jr. (1996). Structure, interactions and dynamics of PRD1 virus I. Coupling of subunit folding and capsid assembly. J. Mol. Biol. *257*, 87–101.

van der Merwe, P.A., McNamee, P.N., Davies, E.A., Barclay, A.N., and Davis, S.J. (1995). Topology of the CD2-CD48 cell-adhesion molecule complex: implications for antigen recognition by T cells. Curr. Biol. *5*, 74–84.

van der Merwe, P.A., Bodian, D.L., Daenke, S., Linsley, P., and Davis, S.J. (1997). CD80 (B7-1) binds both CD28 and CTLA-4 with a low affinity and very fast kinetics. J. Exp. Med. *185*, 393–403.

Viola, A., Schroeder, S., Sakakibara, Y., and Lanzavecchia, A. (1999). T lymphocyte costimulation mediated by reorganization of membrane microdomains. Science *283*, 680–682.

Walunas, T.L., Lenschow, D.J., Bakker, C.Y., Linsley, P.S., Freeman, G.J., Green, J.M., Thompson, C.B., and Bluestone, J.A. (1994). CTLA-4 can function as a negative regulator of T cell activation. Immunity *1*, 405–413.

Wang, J.H., Smolyar, A., Tan, K., Liu, J.H., Kim, M., Sun, Z.Y., Wagner, G., and Reinherz, E.L. (1999). Structure of a heterophilic adhesion complex between the human CD2 and CD58(LFA-3) counterreceptors. Cell *97*, 791–803.

Waterhouse, P., Penninger, J.M., Timms, E., Wakeham, A., Shahinian, A., Lee, K.P., Thompson, C.B., Griesser, H., and Mak, T.W. (1995). Lymphoproliferative disorders with early lethality in mice deficient in Ctla-4. Science *270*, 985–988.

Weiss, A., Manger, B., and Imboden, J. (1986). Synergy between the T3/antigen receptor complex and Tp44 in the activation of human T cells. J. Immunol. *137*, 819–825.

Williams, A.F., and Barclay, A.N. (1988). The immunoglobulin superfamily—domains for cell surface recognition. Annu. Rev. Immunol. *6*, 381–405.

Wülfing, C., and Davis, M.M. (1999). A receptor/cytoskeletal movement triggered by costimulation during T cell activation. Science *282*, 2266–2269.

Protein Data Bank Coordinates

The coordinates of the sB7-1 monomer structure have been deposited in the Protein Data Bank (PDB ID 1DR9).

EXHIBIT 11

The material on this page was copied from the collection of the National Library of Medicine by a third party and may be protected by U.S. Copyright law.

Published by Munksgaard, Copenhagen, Denmark
No part may be reproduced by any process without written permission from the author(s)

A Murine T Cell Receptor Gene Complex: Isolation, Structure and Rearrangement

MARK M. DAVIS, YUEH-HSIU CHIEN, NICHOLAS R. J. GASCOIGNE & STEPHEN M. HEDRICK

INTRODUCTION

The nature of the T cell receptor for antigen has been a major concern of immunologists for many years. Understanding the mechanisms by which T cells learn to recognize self-MHC determinants, how antigen-MHC recognition occurs, and in what forms it can occur is clearly of central importance to understanding T cell differentiation and function. Initially, it was thought that T cells use whole antibodies or portions of antibodies in the recognition and activation process but these ideas were largely disproved by the efforts of many workers (Kronenberg et al. 1980, 1983, Cayre et al. 1981, Nakanishi et al. 1982, Kraig et al. 1983). It was only with the advent of long-term functional T cell lines and hybridomas (as reviewed by Fathman & Frelinger 1983) that the required quantities of homogenous material for both biochemical and genetic studies became available. In the case of murine helper T cells, the advent of cloned cell populations allowed the development of clonotypic antisera (Infante et al. 1982) and, later, monoclonal antibodies (Haskins et al. 1983, Kaye et al. 1983, Samelson et al. 1983) which confirmed the expectation that T cells of different specificities must have distinguishable cell surface determinants. Subsequent immunoprecipitation of the apparent receptor complex with monoclonal antibodies was an important first step in the biochemical characterization of the receptor on these cells, showing a disulfide-linked heterodimer of 80–90 kD which has an alpha and a beta chain of 40–50 kD (Allison et al. 1982, Kappler et al. 1983, Samelson et al. 1983). Similar molecules have also been found on cytotoxic T cells (Staerz et al. 1983) and investigations in both human and murine systems suggest the existence of

Department of Medical Microbiology, Stanford University School of Medicine, Stanford, California 94305 and Department of Biology, University of California, San Diego, La Jolla, California, USA.

Case 1:06-cv-00500-SLR-MPT Document 270 Filed 08/28/2008 Page 26 of 41

The material on this page was copied from the collection of the National Library of Medicine by a third party and may be protected by U.S. Copyright law.

b[illegible]riable and constant peptides (Acuto et al. 1983a, b, MacIntyre & Allison 1983, Kappler et al. 1983).

Our own approach to this problem involved the use of molecular genetic and nucleic acid hybridization procedures to try and isolate candidate gene clones for the receptor molecule and to "work backwards" from such genes to the protein and functional correlations. Because of the power and rapidity of recombinant DNA analysis and related procedures, we believe that this is an important new approach, not only for the isolation of T cell receptor genes but for a wide range of interesting molecules.

Using the combination of strategies reviewed in the following sections, we succeeded in isolating a cDNA clone which encodes a T cell-specific, membrane-associated product, the gene for which is systematically rearranged in a variety of T cell lines and hybridomas, but not in other cells (Hedrick et al. 1984a). This gene exhibited variable, constant and joining region elements remarkably similar in size and sequence to those of immunoglobulin (Hedrick et al. 1984b). A cDNA clone having some of these same properties was also isolated from a human T cell tumor line (Yanagi et al. 1984). The human and the mouse gene are highly

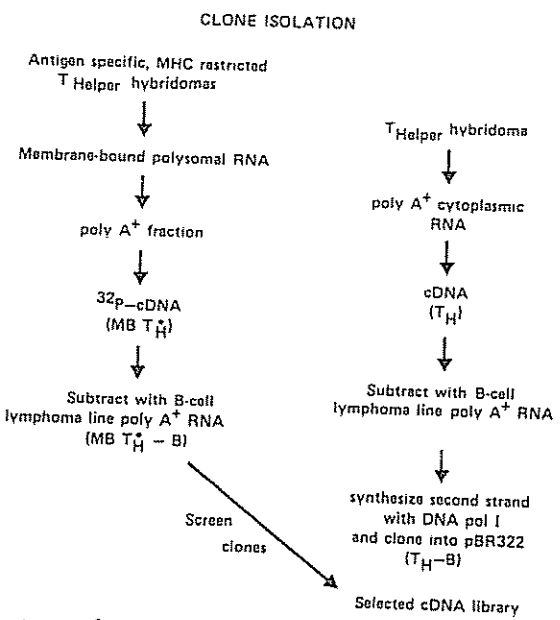


Figure 1. Isolation strategy for cDNA clones encoding T cell-specific, membrane-associated proteins. Adapted from Hedrick et al. 1984a. Subtracted cDNA probes made from the membrane-bound polysomal RNA of T_H hybridomas versus B cell lymphoma mRNA (MB T_H*-B) were used to screen clones from a selected cDNA library (T_H-B).

homologous (82%) in the constant region portion and both appear to [illegible]sent the beta chain of the T cell receptor (Acuto et al. 1984).

THE ISOLATION OF cDNAs ENCODING T CELL-SPECIFIC, MEMBRANE-ASSOCIATED GENES

As indicated above, it has been clear from the work of many laboratories that T cells do not, in general, use antibody genes or segments of genes in any functional context. It was therefore reasonable to assume that T cell receptor messenger RNAs would be expressed in a T cell-specific manner. The importance of this assumption is indicated by the fact that previous studies have shown that B cells and T cells shared a large fraction (98%) of their gene expression (Davis et al. 1982, Davis and Paul unpublished results) and therefore any mRNA that was expressed differently between B and T cells would be enriched substantially by the process of cDNA subtraction. Furthermore, because virtually all known cell surface proteins and most secreted proteins are translated on membrane-bound polysomal RNA, it is possible to achieve an additional fractionation by using that component of the cell for the initial material used to make probes. This strategy is depicted in Fig. 1 (adapted from Hedrick et al. 1984a). Membrane-bound, polysomal mRNAs were prepared as described by Mechler & Rabbits (1981) from antigen-specific, MHC-restricted T_H hybridomas (Kappler et al. 1981, Heber-Katz et al. 1982). Labeled cDNA (MBT_H*) was synthesized and subtracted with B cell lymphoma mRNA as described (Hedrick et al. 1984a). This type of probe was then used to screen a T cell-specific cDNA clone library also made from subtracted material (selected cDNA cloning, Davis et al. 1984), also shown in Fig. 1. A T cell versus B cell (T-B) selection would yield a 50-fold enrichment and a membrane-bound polysomal RNA versus free polysomal RNA fractionation would yield a 3- to 10-fold enrichment based on the measurements of

TABLE I

Expected T cell-specific, membrane-associated polypeptides

Molecule or Complex	Number of Different mRNA Species
T cell receptor for antigen	2
Lyt 1	1
Thy 1	1
L3T4 (±)	1
T3 (?)	3
Interleukin 2 (?)	1
B cell growth factor (?)	1
Total known markers	10
Estimated from hybridization measurements	40–70
cDNA clones isolated to date	16

Case 1:06-cv-00500-SLR-MPT Document 270 Filed 08/28/2008 Page 27 of 41

The material on this page was copied from the collection of the National Library of Medicine by a third party and may be protected by U.S. Copyright law

Hedrick et al. (1984a). So a combination of these two selections would yield between a 150- and a 500-fold enrichment for T cell receptor messenger RNA as well as other cell surface and secreted species. Table I shows the T cell-specific cell surface markers that are known to be specific to T helper cells and hybridomas and which may be present in the MBT_H*-B fraction. These include the murine T3 by analogy to the work done in the human system (and the recent work of Lanier and Allison in the mouse, personal communication, Samelson & Schwartz, this volume), the L3T4 helper cell marker, Thy 1 and the presumptive two chains of T cell receptor for antigen. It is not clear if the factors indicated (IL-2 and BCGF) are expressed in the unstimulated cells that we have used but they may be present in small amounts. We estimate from the cDNA kinetic measurements and the mass measurements that approximately 70 genes would be both T cell specific and on membrane bound polysomes (Hedrick et al. 1984a). From the various considerations presented in that reference, a lower limit might be 40 different genes. This disparity between the estimated number of genes expressed in this category (40–70) and what is probably an overestimate of the number of known markers (10) is an important indication of our ignorance regarding the genetics of these cells. In all, 10 different genes were isolated in the first screening by the strategy shown in Fig. 1. These cDNA clones, and their respective mRNA sizes in Northern blot analysis are shown in Table II. The cloning frequences will be discussed in the next section. Preliminary results from our laboratory indicate that we have isolated perhaps six new genes that are both T cell-specific and membrane-associated (Becker et al., work in progress). An important feature of this gene isolation was the internal control of screening for the Thy 1 gene using a rat cDNA probe isolated by Silver and his colleagues (Moriuchi et al. 1983). This probe indicated that one of the clones shown in Table II, TM8, is in fact a mouse Thy 1 cDNA clone and that therefore the selections were successful

TABLE II

Clone	mRNA size (kb)	T-B Library (Frequency/20)	Thymus Library
TM4	1.5,1.9,4.0,5.0	0.003%	0.014%
TM8	1.9	0.001%	0.002%
TM26	1.0	N.D.	N.D.
TM28	1.6	N.D.	0.038%
TM30	0.7	N.D.	N.D.
TM32	0.6	N.D.	N.D.
TM33	1.7,1.9,3.0	N.D.	<0.005%
TM86	1.0,1.3	0.01%	0.17%
TM90	1.7	N.D.	0.12%
TM97	1.8,1.9	0.001%	0.01%

N.D. = not determined.

(Hedrick et al. 1984a). Subsequent DNA sequence analysis confirms this supposition (R. Germain, personal communication). These data indicate that there is a substantial fraction of T cell-specific gene expression for which no known serological markers are in hand and that this methodology is useful in approaching them. Recent advances in genetic engineering have made it possible to express large quantities of protein either alone or in the context of bacterial proteins such that it should now be possible to take many of these unknown genes that we have isolated in this category and generate antisera or monoclonals to them, or in the case of possible growth factors, develop assay systems. It was also clear that this strategy offered an attractive alternative to classical procedures towards the isolation of T cell receptor genes.

ISOLATION OF RARE ABUNDANCE CLASS MESSENGER RNAs AND RECEPTOR GENE EXPRESSION

The intensity of Northern blot hybridization with many of the T cell specific cDNA clones indicated that some were very rare. This is not unexpected as a number of reports in the literature have indicated that the limiting step in screening clones with labeled cDNA probes is the percentage of the probe which contains the species of interest. Specifically, Dworkin & Dawid (1980), in a reconstruction experiment, found that they were unable to detect ovalbumin cDNA clones if less than 0.06% of their probes contained ovalbumin. Similarly, Crampton et al. (1980) set 0.05% to 0.2% as the detection limit in plasmid library screening. Since most genes (approximately 95% [Lewin 1980]) are in the rare abundance class (approximately 0.001–0.005%), they are effectively undetectable when screening with unfractionated cDNA probes. Subtraction procedures such as those used here, however, should greatly enrich for the species of interest. In this case, since the set of genes which is T cell-specific and on membrane-bound polysomal RNA is only 0.5% of the cytoplasmic poly A^+ messenger RNA (Hedrick et al. 1984a), probes corresponding to this difference should be 200-fold enriched for the relevant sequences. Thus, even very rare genes should behave as if they were abundant ($200 \times 0.002 = 0.4\%$).

To explore this further, we estimated the cloning frequencies of a number of the less abundant TM (T cell-specific membrane-associated) cDNA clones. The inserts of these clones were labeled and hybridized to both the original T-B library (Hedrick et al. 1984a) and to an unselected library made from whole thymocyte RNAs by Dr. C. Benoist. The resulting frequencies are shown in Table II, with the frequency of positive clones in the T-B library divided by 20, for the estimated enrichment of T cell-specific sequences (Hedrick et al. 1984a). Approximately 5,000 clones were screened in the T-B library and 100,000 in the thymocyte library. The results indicate that we are able to isolate apparently very rare genes; especially the presence of at least three of the TM series cDNA clones

Case 1:06-cv-00500-SLR-MPT Document 270 Filed 08/28/2008 Page 28 of 41

The material on this page was copied from the collection of the National Library of Medicine by a third party and may be protected by U.S. Copyright law

in a .001–0.003% range supports the initial contention. Another interesting point is that several other clones shown in Table II have a significantly lower level of expression in the T_H hybridoma versus the thymocyte library, including TM86. As will be discussed further, TM86 is the beta chain of the T cell receptor. It is interesting that the expression of the receptor is so high (0.2%) in thymocyte RNA compared with that of the 3.3T T_H hybridoma (0.01%). It has been confirmed by Northern blot analysis of RNAs and in the cloning frequencies from other cDNA libraries (in particular, an unselected library of the T_H hybrid, 2B4, has a frequency of this chain of 0.02%) that this low level of expression is typical of hybridomas. This disparity between thymocyte and hybridoma expression appears to represent a problem specific to T-hybridomas since cDNA libraries made from four different T_H lines contain clones of this chain of the receptor at a frequency of 0.1–0.4% (P. Patten et al., work in progress). Also a library made from Con A-stimulated spleen cell RNA (the kind gift of C. Benoist) contains 0.2% receptor-positive clones (S. Hedrick and M. Davis, unpublished

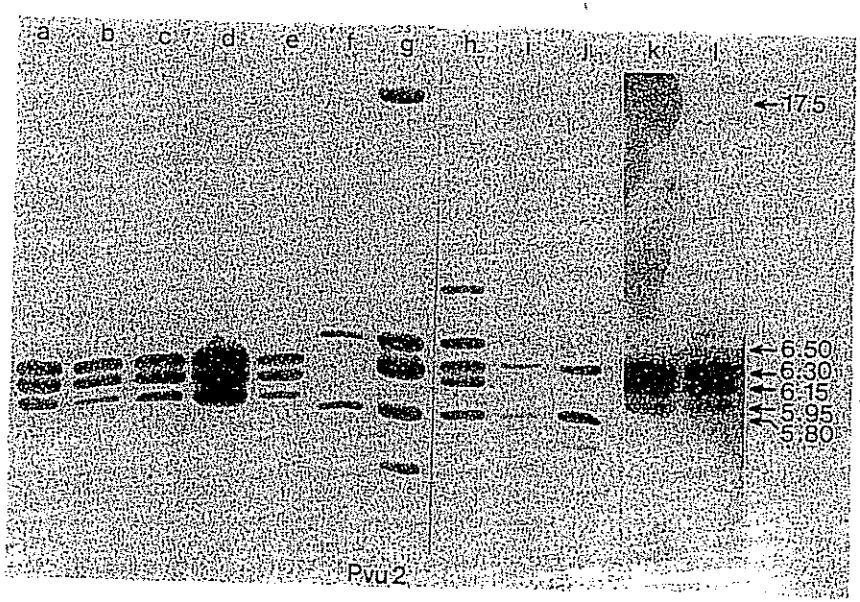


Figure 2. Southern blot analysis showing rearrangement of the T cell receptor gene in DNA from T cells (lanes f-j) but not in a B cell (k) macrophage (l) or liver (a-e) DNAs. DNA was digested with the restriction enzyme PvuII. Lanes a-e are liver DNAs from BALB/C AKR, B10.A (2R) and B10.A (5R) strains of mouse, respectively. F is BS5147. 2B4 and M12 are cytochrome reactive T_H hybrids, 3.3T responds to amidated cytochrome and GAT responds to a peptide. K is a B cell lymphoma line (BS-4) and l is a macrophage line, P388D. (These latter two DNAs were the kind gift of Dr. F. Melchers).

results). Taken together, this indicates that the typical level of expressio. a normal T cell of this gene is 0.1–0.2% of the mRNA, and that hybridomas and at least some lymphoma lines have a 10-fold reduced level of expression. This may be due to instability of the receptor in tumor lines and hybrids or the regulation of this gene in differentiation.

SOMATIC REARRANGEMENT AND T CELL SUBSETS

Of primary importance for assessing whether one of the selected genes could encode a T cell receptor for antigen was to demonstrate that there had been somatic rearrangement of the gene during T cell differentiation. This derives from the fact that rearrangement in immunoglobulin genes is responsible in large part for the the great diversity that is seen in antibody specificities (Tonegawa 1983). Therefore we surveyed seven of the T cell specific cDNA clones in Table II for rearrangement using Southern blot analysis (Hedrick et al. 1984a). Only one, TM86 was arranged differently in liver DNA versus various T cell DNAs. Fig. 2 shows these rearrangements. Three distinct bands are evident in this Pvu II digest. Whereas differing mouse strains show identical patterns, every T cell line or hybrid shows unique bands, indicating some systematic rearrangement of this gene. The B cell and macrophage line DNA's shown are identical to the liver pattern, indicating the tissue specificity of this process. Also interesting to note from Fig. 2 is that the BW5147 pattern is distinctly rearranged from the germline pattern, and that all of the hybrids in the figure retain this pattern of bands. Subsequent analysis had indicated that 28 out of 30 BW5147 fusions retain both of these bands and that the two exceptions retain the uppermost one. These observations led to the suggestion (Hedrick et al. 1984a) that the BW5147 rearrangement is under a particularly strong selection to be retained in the hybrid and that perhaps this could be related to oncogenesis, such as the oncogenic translocation which occurs in many B cell-derived tumors (Shen-Ong et al. 1982).

Rearrangement of this locus in a variety of T cell types has been observed as summarized in Table III. It indicates that all the T_H cell lines or hybridomas (14) show at least one distinct rearrangement other than that of BW5147. Similarly, a number of cytotoxic T cell lines and hybrids (5 out of 6) also show evidence of rearrangement. In contrast, very few (2 out of 19 of the T suppressor hybridomas obtained from various sources) show a non-BW, nongermline arrangement using

TABLE III

Rearrangements in functional T cell lines and hybrids

	T helpers	T cytotoxic	T suppressors
Lines	4/4	4/4	1/1
Hybrids	10/10	2/2	2/19

Case 1:06-cv-00500-SLR-MPT Document 270 Filed 08/28/2008 Page 29 of 41

The material on this page was copied from the collection of the National Library of Medicine by a third party and may be protected by U.S. Copyright law

this probe. This indicates that both cytotoxic T cells and helper T cells utilize this gene complex and that suppressor T cell hybridomas are somehow different: either they utilize some other locus or they employ a more nonspecific mechanism of action. There is further uncertainty as to this question because of the one suppressor line indicated in Table III that is rearranged (Patten et al., unpublished results) and in reports of antigen-specific human suppressor lines which rearrange and express receptor genes (T. Mak, personal communication). This observed discrepancy may represent some fundamental differences in the human and murine suppressor systems. This will be an important question to resolve because, if all T cells utilize the same recognition structure, then isotypes as they exist in immunoglobulins will not be relevant and accessory molecules such as Lyt 2 and L3T4 might play the major roles in defining T cell function.

HOMOLOGY TO IMMUNOGLOBULIN VARIABLE, JOINING AND CONSTANT REGION ELEMENTS

Using the TM86 probe, a nearly full length cDNA clone was isolated from a thymocyte cDNA library (86T1). Sequence analysis indicated a long open reading frame of 306 amino acids and this predicted protein sequence was used to survey the Dayhoff database, using the search program of Wilbur & Lipman (1983). Of the top 25 scores in this homology search routine, 24 corresponded to immunoglobulin variable and constant region genes from a variety of different species (Hedrick et al. 1984b). Thus this molecule is more homologous to immunoglobulins than to any other known protein. The protein sequence homology to immunoglobulin variable and constant region elements ranges from 20–40% and has been described for both mouse (Hedrick et al. 1984b) and human sequences (Yanagi et al. 1984). In order to determine whether in fact there were independently assorting gene elements composing the messenger RNA that was sequenced, we have characterized a variety of different cDNA clones by restriction mapping and sequence analysis and these are shown in Fig. 3. It was apparent that while the 3′ portion of the molecule was highly conserved or nearly identical between the different cDNA clones, the 5′ portion was not, thus corresponding to the constant and variable regions of immunoglobulins. Also interesting was the fact that in two separate examples, a 16 amino acid element between the putative variable and constant regions was present in some cDNA clones but not in others. This indicates that, like immunoglobulin J regions, these elements have the ability to assort independently. In addition, these elements have a significant amino acid homology to immunoglobulin J's (Hedrick et al. 1984b, Yanagi et al. 1984). This analysis also indicated that two very similar but distinct constant regions were being expressed: C_T and C_T' (Chien et al. 1984, Gascoigne et al. 1984). One form (C_T) predominates among the thymus-derived clones (86T series) that we have isolated and the other (C_T') seems most often expressed in

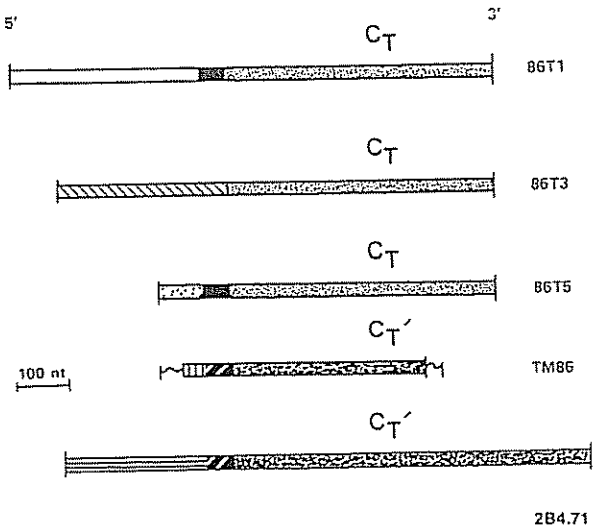


Figure 3. cDNA clone homologies. 86T1, 86T3 and 86T5 were described previously and derived from a thymocyte cDNA library (Hedrick et al. 1984b). TM86 was described in the same publication and derives from the helper hybridoma, 3.3T (Heber-Katz et al. 1982). 2B4.71 is the expressed gene of the helper hybrid 2B4 (Samelson et al. 1983), the isolation and sequence of which is described in Chien et al. (1984). C_T and C_T' refer to the first and second constant region loci, see later sections.

functional lines and hybridomas. This significance of these findings is not yet clear.

V_T STRUCTURE: POSSIBLE FRAMEWORK AND HYPERVARIABLE REGIONS

Analysis of homologies within the variable regions of heavy and light chain immunoglobulins defined "hypervariable" and "framework" portions (Kabat et al. 1983). The three hypervariable regions of both heavy and light chain V regions type were predicted to be involved in antigen binding. Subsequent X-ray crystallographic analysis in fact showed that these regions formed loops which can directly contact specific antigens (Amzel et al. 1974, Davies et al. 1975). Similarly, analysis of T cell receptor variable region homologies should be informative about the general nature of the binding site and might usefully predict which regions are most important. Three probably functional $V_T\beta$ sequences have now been published, two in the mouse (Hedrick et al. 1984b, Chien et al. 1984), and one in the human (Yanagi et al. 1984). All of these have significant (20–35%) homology to immunoglobulin heavy and light chain variable regions (Yanagi et al. 1984, Hedrick et al. 1984b). These sequences are somewhat more homologous

Case 1:06-cv-00500-SLR-MPT Document 270 Filed 08/28/2008 Page 30 of 41

The material on this page was copied from the collection of the National Library of Medicine by a third party and may be protected by U.S. Copyright law.

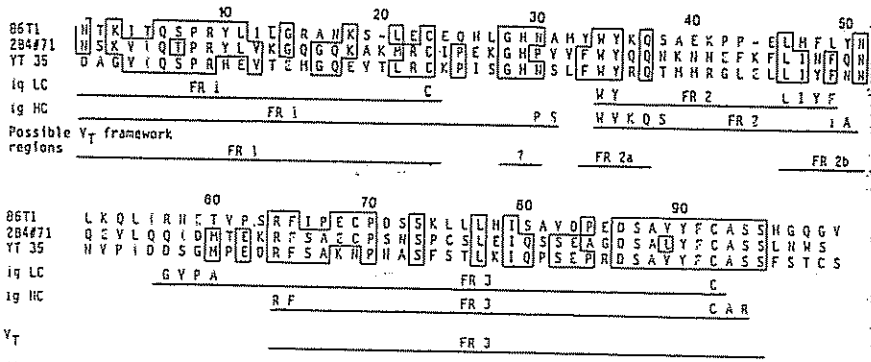


Figure 4. V_T homologies and possible framework regions. Three different V_T gene segments are compared and analyzed with respect to heavy and light chain framework (FR) regions (Kabat et al. 1983). Letters on top of the immunoglobulin framework borders indicate common residues in those regions.

to each other, as shown in Fig. 4. These homologies range from 35–45% and the human sequence (YT35) is more homologous to one of the mouse sequences (2B4.71) than the two mouse sequences are to each other.

Although the number of sequences is too small to compute a meaningful variability plot (Wu & Kabat 1970), it seems reasonable to compare the homologies observed in Fig. 4 to the heavy and light chain framework regions, especially where the border regions of immunoglobulin frameworks are homologous to the conserved residues in the T cell molecule. The conserved sequences at the edges of the Ig frameworks and the frameworks themselves are shown in Fig. 4. The best example of how one can attempt to predict V_T framework regions is illustrated by the case of the Ig framework 3 where the position of the homology region (in the V_T's), as well as the bordering residues on either side, are consistent with a framework region more similar to FR-3 of heavy chains than to that of light chains. This is perhaps not so surprising given the fact that both heavy chains and the T cell genes shown here utilize D region segments immediately adjacent to this region (Chien et al. 1984, see later sections) and light chains do not. Somewhat less clear is the placement of FR-1, but since we do not see continuous homology past the first cysteine, we propose that this framework region corresponds best to that of the light chain immunoglobulin. This analysis starts to reveal differences between Ig and the T cell variable region around Framework 2. While the edges of FR-2 are highly conserved, the 5′ portion with both heavy and light chain and the 3′ end with light chain (the sequence LIVY is the same between YT35 and the light chain consensus sequence in Fig. 4), the central seven amino acids are not conserved at all between the three T cell receptor sequences. This is even more striking since this region (FR-2) is the most highly conserved of all the immunoglobulin frameworks (Kabat et al. 1983). Because of the large non-homologous region between the conserved residues, this portion of V_T may represent a new hypervariable region, perhaps in addition to ones in the traditional places or, as indicated by the anomalous short conserved sequence between FR-1 and FR-2, it may represent a re-positioning of HV-1. Many more sequences and structural work will be necessary to test this possibility. It does, however, suggest that while the overall structure of the binding site (as judged by putative framework and hypervariable regions) may be very similar to that of immunoglobulins, there may be some profound differences. In particular, one would expect a slightly different configuration of the site, perhaps to more easily accommodate the combined MHC-antigen determinants. Because of the fact that monoclonal antibodies in at least some cases can recognize both antigen and MHC class I determinants (Sherman et al. 1983) and because of the significant homology to Ig V regions mentioned, one would not predict a totally different type of binding site, but some altered configuration may predominate.

GENOMIC ORGANIZATION AND REARRANGEMENT

In order to examine the germline arrangement of the elements which give rise to this chain of the T cell receptor, Chien et al. (1984) isolated a series of genomic clones from liver DNA and the T_H hybridoma, 2B4. These are illustrated in Fig. 5. Analysis of the liver DNAs covering the constant region locus (Fig. 5b) (Chien et al. 1984, Gascoigne et al. 1984) indicate a tandem array in the form (J_T1-7 – C_T) (J_T1-7′ – C_T′). We have adopted the C_T, C_T′ nomenclature to avoid confusion

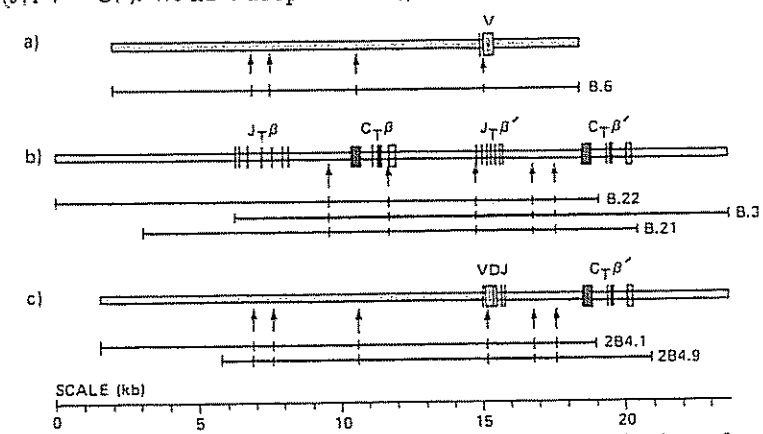


Figure 5. Genomic organization and rearrangement in the constant region locus. J_T and C_T coding segments were identified on approximately 15 kilobases of DNA (Chien et al. 1984, Gascoigne et al. 1984) and are shown in b. A germline V_T gene, shown in a, was found rearranged to the second constant region locus (J_T′–C_T′) in the active gene of the hybridoma 2B4 (Chien et al. 1984). Arrows (↑) indicate EcoRI sites.

Case 1:06-cv-00500-SLR-MPT Document 270 Filed 08/28/2008 Page 31 of 41

The material on this page was copied from the collection of the National Library of Medicine by a third party and may be protected by U.S. Copyright law.

with the four different exons of the constant region (e.g., C_T1, C_T2 or $C_T\beta1$, $C_T\beta2$, making use of the immunoglobulin convention). Evolutionarily this arrangement as seen in Fig. 5b, is a mixture of the lambda light gene organization ($(J\lambda I\text{-}C\lambda I)$ $(J\lambda II\text{-}C\lambda II)$ with the large array of J regions in kappa light chain and heavy chain genes (Tonegawa 1983). The intron-exon structure and the use of D (diversity) elements is much like that a heavy chain genes. The J region clusters and the C region organization will be discussed in separate sections following this one. The rearrangement of this locus in the 2B4 line also appears very much like that of immunoglobulins, with a separate V region and its 5′ flanking sequences (Fig. 5a) brought adjacent to a J_T element and its 3′ flanking sequences (Fig. 5b), resulting in the apparent active gene (Fig. 5c). Another 2B4-specific rearrangement of this locus was also isolated and appears to be non-functional (D. Becker et al., work in progress). That the one shown in Fig. 5c is the functional rearrangements supported by the following criteria:

1.) The rearrangement shown in Fig. 7b is contained on a large (17.5 kb) Pvu II restriction fragment (Fig. 2) which has also been seen in Southern blot analyses of three other cytochrome *c*-specific hybridomas, but not in lines with other antigenic specificities (Hedrick et al. 1984c).

2.) The variable region joined to the J_T cluster shown in Fig. 7b has been subcloned and shown to hybridize to mRNA from six different cytochrome *c* reactive lines, but not to others (Hedrick et al., work in progress).

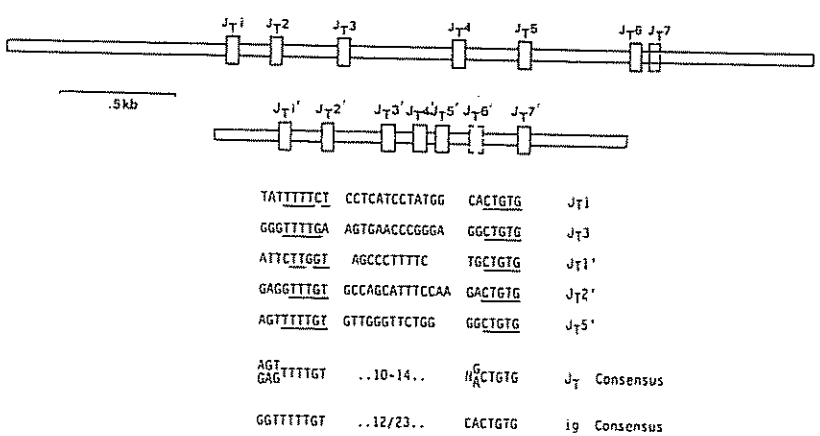


Figure 6. J_T organization and 7 and 9 nucleotide elements.

a. The two separate joining region clusters, J_T1–7 and J_T1–7′. Dashed lines indicate pseudogenes, although others may be nonfunctional as well.

b. Sequences immediately 5′ to each of the five J_T elements known to be functional (with respect to rearrangement). Approximate consensus sequence compared with that of immunoglobulins.

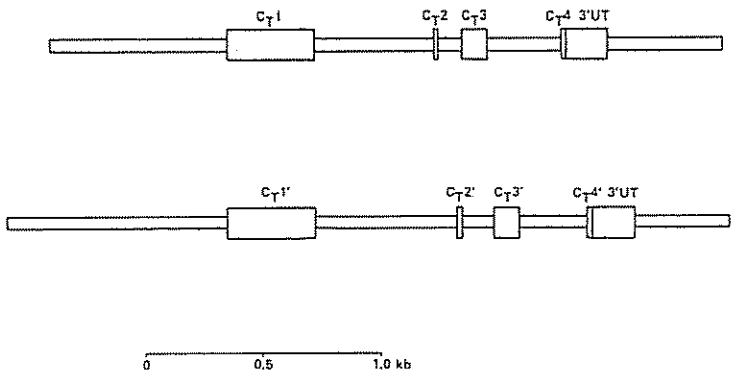


Figure 7. C_T intron/exon structure. Organization of C_T and C_T' (see text).

3.) The two rearrangements characterized constitute all of the non-BW5147-derived bands which appear in Southern blots (Fig. 2) and only that shown in Fig. 7b contains a variable region.

The analysis of this rearranged gene from 2B4 indicates that, just as in the case of immunoglobulins, separate V, J and D (as will be discussed later) region elements are recombined adjacent to a constant region gene segment. An RNA transcript of this recombined gene is then presumably spliced to produce the observed mRNA (Chien et al. 1984). Another important observation stemming from the analysis of this gene is the apparent absence of somatic mutation in the variable region exon. The implications of this are discussed in the last section.

J REGION GENOMIC STRUCTURE AND SIGNAL SEQUENCES FOR SOMATIC RECOMBINATION

Chien et al. (1984) and Gascoigne et al. (1984) have isolated and sequenced two distinct, but closely linked J_T clusters (J_T and J_T'), which appear to provide all of the five J region elements thus far identified from cDNA clones (Fig. 3 and unpublished data). Together, these two clusters may encode as many as 12 functional J_T elements, more than any known immunoglobulin cluster (which range from four to six) (as reviewed in Kabat et al. 1983), thus doubling or possibly tripling the amount of diversity available from these elements. The structure of these two clusters and the 5′ flanking sequences for those J_T elements known to be functional are shown in Fig. 5. The latter are especially important because they exhibit a very marked similarity to the 5′ flanking sequences of immunoglobulin J regions, in particular the 7 and 9 nucleotide conserved sequences thought to be involved in the somatic recombination event (Sakano et al.

Case 1:06-cv-00500-SLR-MPT Document 270 Filed 08/28/2008 Page 32 of 41

The material on this page was copied from the collection of the National Library of Medicine by a third party and may be protected by U.S. Copyright law

19 lax et al. 1979, Tonegawa 1983). This indicates that the basic mechanisms underlying the DNA splicing events associated with variable region formation are very similar if not identical between this T cell gene and immunoglobulins. That they may not be interchangeable is evidenced from the consensus sequence differences shown in this figure and the fact that the G in the first position of the 7-mer in three cases is never found in that position in immunoglobulin 7-mers (Chien et al. 1984). Also significant is the average spacing between the 7 and 9 nucleotide elements (12–13 nucleotides) which is also consistent with immunoglobulins, especially the 12/23 rule discussed in a later section.

CONSTANT REGION GENOMIC STRUCTURE

As indicated in Fig. 5b, two distinct but very similar constant region gene segments were found in the genomic clones. Both of these are expressed in functional mRNA (Fig. 3, Chien et al. 1984). Remarkably, these two constant regions differ by only four amino acids, and all of these differences occur in the carboxy-terminal region of the predicted protein structure (Chien et al. 1984, Gascoigne et al. 1984). The intron-exon structure of these constant regions is shown in Fig. 6 (Gascoigne et al. 1984). The constant region is composed of four distinct exons; C_T1, an external domain which encodes the first 125 amino acids of the region and is analogous to the typical globular domain of immunoglobulins. C_T2, a mini-exon of six amino acids which contains the last cysteine residue of the molecule which we have postulated to be involved in the linkage to the other chain (alpha) of the heterodimer. This exon also has some similarity to the hinge region of heavy chain Ig (Gascoigne et al. 1984). C_T3, encodes 36 amino acids which have a significant hydrophobic character (Hedrick et al. 1984b) and probably constitute the trans-membrane portion; finally, C_T4 encodes five amino acids which contain three positive charges in a row and may serve to anchor the molecule on the cytoplasmic side. The 3′ untranslated region is joined directly to the last coding region (C_T4) as in the case of membrane $C\mu$ (Early et al. 1980b).

As mentioned before, these two constant regions are very highly conserved with respect to coding region sequences and all of these changes are in the two carboxy terminal exons. In particular, there are three amino acid chains in C_T3 and one in C_T4, the trans-membrane and cytoplasmic exons, respectively. In contrast to this conservation, the 3′ untranslated regions are almost completely divergent (<50% homologous) indicating that these genes duplicated over 120 million years ago (Gascoigne et al. 1984). This and the fact that the constant region is so similar between mouse and human (82%, Williams 1984) indicates that the T cell receptor beta chain is very strongly conserved in evolution. Also interesting is the fact that there is only one nucleotide difference between the two C_T1 exons (of 375 nucleotides) which means that a recent gene conversion event must have taken place between those two exons (C_T1 and C_T1') (Gascoigne et al. 1984). This strong conservation of the coding region sequence may ex why it has been so difficult to obtain allotypic antisera or monoclonals for the receptor.

D REGION ELEMENTS AND THE "12/23" RULE

Analysis of the rearranged gene discussed above and the relevant precursor gene segments from liver DNA (Chien et al. 1984) indicated that 8 nucleotides between V_T and J_T could not be accounted for and an additional "D" element was postulated. Supporting this contention is the similar analysis of a human V region sequence (Siu et al. 1984). Data concerning the independent assortment of D region elements has also been obtained (P. Patten and M. Davis, unpublished results). Most significantly, however, we have recently isolated and sequenced an unrearranged D_T region element (Kavaler et al. 1984). This murine D region was located several hundred nucleotides 5′ to the J_T cluster of Fig. 5, similar to the case of D_{Q52} near the J_H cluster (Sakano et al. 1981). This element is flanked by 7 and 9 nucleotide sequences spaced by one or two turns of the DNA helix, just as are D regions in immunoglobulin heavy chain genes (Kurosawa & Tonegawa 1982). The essentials of this finding and the comparison to V_H, D_H and J_H elements are shown in Fig. 8. Two important points are evident:

1.) The "11/22" or "12/23" rule (Early et al. 1980a, b) is preserved in the formation of the T cell variable region, just as it is in immunoglobulins. This again points out the fact that identical or nearly identical mechanisms must be operating in the rearrangement of these genes.

2.) In addition, while the 12/23 rule appears to exclude direct V_H–J_H joining in immunoglobulins, it would not exclude such an event in the T cell receptor gene segments. Although we have yet to see a case of such joining in the sequences of more than 10 VDJ junctions (unpublished data), it could possibly be important

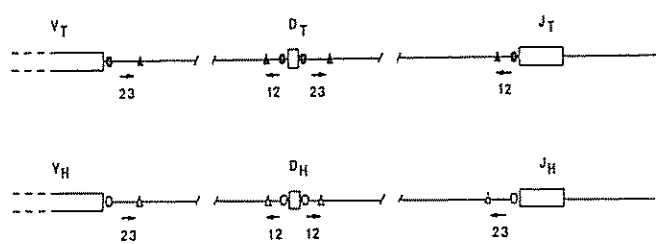


Figure 8. V, D and J region elements in the T cell receptor beta chain gene and in IGH, the immunoglobulin heavy chain locus. Schematic presentation of the 12 or 23 nucleotide spacing found between the 7 (○ ●) and 9 (△ ▲) nucleotide conserved sequences thought to be involved in variable region formation. Orientation of these elements is indicated by arrows (→).

Case 1:06-cv-00500-SLR-MPT Document 270 Filed 08/28/2008 Page 33 of 41

The material on this page was copied from the collection of the National Library of Medicine by a third party and may be protected by U.S. Copyright law.

in terms of extra variation in the V region. Alternatively, some constraint other than the 12/23 rule might prevent the bypassing of the D region elements.

Another interesting possibility is that D-D joining may be permissible (Siu et al. 1984, Kavaler et al. 1984), which might also contribute significantly to V region diversity.

Another indication of the shared machinery for recombination between B cells and T cells is the relatively frequent instance of aberrant rearrangement of the IgH locus in T cells. In particular, Sakano et al. (1981) characterized several D_H–J_H joining events in T cell tumors. This phenomenon now seems explicable in terms of "cross-talk" between enzymes which may have been turned on to rearrange T cell receptor genes and can, at least partially, act on immunoglobulin genes.

CHROMOSOMAL LOCALIZATION

Mapping studies attempting to define the chromosome(s) encoding the T cell receptor molecules have been the subject of continual controversy (Coutinho & Meo 1983). Because of the antibody paradigm, attention focused initially on the IgH locus of chromosome 12 (in the mouse) where anti-idiotypic sera appeared to link the T cell specificity to this region (Binz et al. 1976, Eichman & Rajewsky 1977). More recent evidence concerning T cell-specific surface antigens which are closely linked to IgH also raised the possibility of functional linkage to the heavy chain locus of immunoglobulin (Owen & Riblet, 1984). In order to help resolve this controversy, our group (Lee et al. 1984) and others (Kronenberg et al., personal communication) have mapped the beta chain receptor gene to mouse chromosome 6, in the vicinity, but not closely linked to, the Igκ locus. That this association is not obligatory is evidenced by the fact that the human equivalent of this gene maps to chromosome 7 in that species (T. Mak, personal communication) which is not one of the Ig-bearing chromosomes. This loose linkage to the kappa locus is an additional indication of the shared evolutionary origins of this T cell receptor gene and immunoglobulins. The recombinant inbred linkage studies cited earlier (Epstein et al. 1984) also indicate that the beta chain locus is a considerable distance from Igκ ($\sim$10cM).

PREDICTED PROTEIN STRUCTURE

The proposed beta chain protein structure is shown in Fig. 9a, with leader (L), variable (V), diversity (D) and joining region (J) elements attached to either of two very similar constant (C) regions. The external (Ext), hinge (H), transmembrane (TM) and cytoplasmic (Cyt) portions of the constant region are discussed in a previous section and in Gascoigne et al. (1984). The cysteine residues shown in Fig. 8 could form two globular domains by analogy to immunoglobulin; also, the additional cysteine residues internal to each domain might form an intra-chain bond as proposed for similar residues in the rabbit (McCartney-Francis et al. 1984). The last cysteine, in the hinge region, has been proposed as the principal bridge to the other chain (Hedrick et al. 1984b). If the leader polypeptide is cleaved after amino acid 19 as shown, then the processed protein would be 32.1 kD prior to glycosylation. This value compares favorably to that obtained by Kaye & Janeway (1984) in tunicamycin studies of the murine receptor (31 kD), as well as those obtained by Samelson & Schwartz (this volume) using a glycosidase (32–34 kD) and to the 32–34 kD values of Terhorst (1984) (also using glycosidases) in the human system. There are five potential N-glycosylation sites in the constant region of the 86T1 murine beta chain (Hedrick et al. 1984b) and four in the 2B4.71 protein (Chien et al. 1984). The human beta chain has two, well-characterized glycosylation sites (Terhorst 1984) confirmed by the sequence of Yanagi et al. (1984).

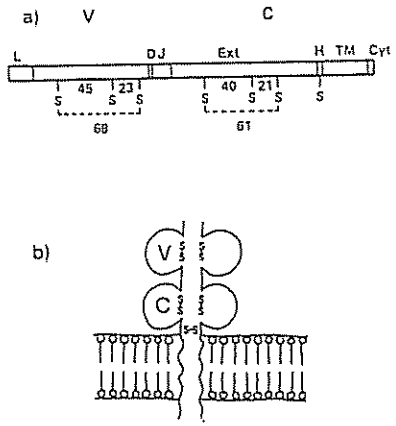


Figure 9. Predicted protein structure of the β chain subunit. S-S indicates predicted sulfhydral bonds based on the analogy to immunoglobulins. Leader (L), diversity (D) and joining (J) region elements are shown within the variable region domain (V). External (Ext), hinge (H), trans-membrane (TM) and the cytoplasmic terminus are shown within the constant (C) region.

GENERATION OF DIVERSITY AND ANTIGEN-MHC RECOGNITION

As seen in the previous sections and judging from our unpublished data, the number of possible beta chain polypeptides seems very extensive. We have sequenced portions of eight distinct V_T elements in the murine system (Hedrick et al. 1984b, Chien et al. 1984, Patten et al., manuscript submitted), eight probable D_T regions (*op. cit.*, unpublished results) as well as 12 potentially functional J_T

Case 1:06-cv-00500-SLR-MPT Document 270 Filed 08/28/2008 Page 34 of 41

The material on this page was copied from the collection of the National Library of Medicine by a third party and may be protected by U.S. Copyright law

...as (Chien et al. 1984, Gascoigne et al. 1984). These elements alone could generate almost 800 different possible V region exons, added to which is the contribution of joining at different parts of the same element and reading out of frame in the case of D regions (Hood et al. 1980, Tonegawa 1983). Although V_T regions do not appear to occur in the large cross-reactive families (Patten et al., manuscript submitted) that are the case with heavy chain and kappa light chain Igs, there could easily be many more V_T regions and D_T regions. Together, these considerations indicate that there are probably many thousands, perhaps tens of thousands of possible versions of this polypeptide, comparable to the diversity of Ig heavy chains. Since the alpha chain also has variable and constant portions (Acuto et al. 1983b, Kappler et al. 1983, MacIntyre & Allison 1983), the number of potential binding sites probably compares very favorably to those of immunoglobulin (if the two chains fold together to form a single site). If the alpha chain gene also has D region elements, it is conceivable that the number of potential sites could be even greater.

Jerne (1971) and others have proposed a major role for somatic mutation in T cell receptor maturation, as a means of adapting to self-MHC receptors to antigenic determinants. However, when comparing the liver DNA-derived V_{T2B4} gene segment to its expressed counterpart, no evidence of somatic mutation was seen (Chien et al. 1984). Furthermore, a number of independently derived cDNA clones sharing the same V_T region have thus far shown very few sequence differences either (Chien et al., work in progress). While these limited data do not exclude some role for somatic mutation in the generation of diversity of these receptors, they do indicate that it might be on the same, somewhat limited scale as that of immunoglobulins (Tonegawa 1983), or absent altogether.

Despite this apparent lack of somatic mutation, however, the arguments summarized above indicate that the number of possible receptor binding sites seems likely to be very large. Given that this is true, two apparent contradictions with current beliefs need to be explained: 1) That since cellular immunity appears to preceed humoral (antibody-mediated) immunity in evolution, the T cell receptor must represent a more primitive (i.e. simpler) form of recognition. The probable explanation for this is simply parallel evolution, in that while the "original" receptor gene almost certainly is more primitive that what we are seeing in mammals, it has had ample time to become more sophisticated. It also seems reasonable to propose that both the J and the D region elements of immunoglobulins and the mechanism for rearranging them derive from the gene studied here. 2) Numerous studies, particularly those of the flu virus (Gearhart and Meichers, personal communication) indicate that T cells can recognize only a fairly narrow range of determinants in cases where B cells (antibodies) can recognize a large number. In view of the data discussed here, the probable explanation for this apparently small repertoire size is not the genetic machinery of the T cell receptor *per se* but that the requirement for MHC co-recognition in the same binding site must limit the number of useable products (see following discussion).

The data summarized in Fig. 9a, as well as the genomic organization covered in the earlier sections, indicates that this subunit of the T cell receptor is very much like an immunoglobulin light or (particularly) heavy chain. This being the case, it seems very likely that the other chain of the receptor must also resemble immunoglobulin. The consequences of this reasoning are indicated in Fig. 9b (after Williams 1984) in the, by now obligatory, shorthand of immunoglobulin "superfamily" related molecules. Thus it has been predicted (Williams 1984, Chien et al. 1984) that the variable regions of the alpha and beta chains will interact to form a single combining site. This is even more likely considering the basic similarities of the apparent framework-hypervariable region structure, even taking into account the differences in FR-2 (Fig. 4). Thus, the data discussed here strongly support the one-receptor model of antigen-MHC recognition, as does much of the recent cellular data (for example Kappler et al. 1981). In addition, the previously mentioned work of Sherman et al. (1983), sets a precedent in their finding that at least some antibody molecules can recognize both antigen and MHC determinants.

If there is only one binding site, how is the predisposition towards self-MHC "learned" in the thymus prior to antigenic exposure? One possibility proposed in Chien et al. (1984) is illustrated in Fig. 10, which depicts the range of T cell receptor dissociation constant's (Kd's) for a given self-MHC determinant. If only those cells bearing receptors which fall into the "hypothetical window" shown in this figure (representing relatively weak binding sites) were permitted to leave the thymus, then cells with only partially filled receptor sites would be selected for. These partially filled sites might then be completely filled by antigen-MHC determinants, presumably resulting in a stronger binding constant (hence lower

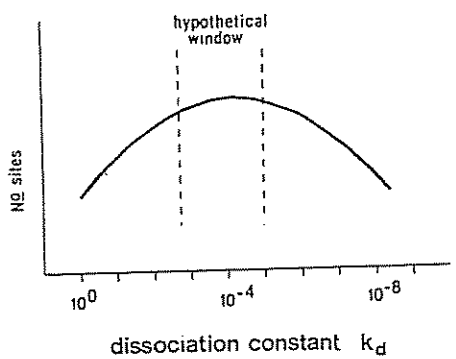


Figure 10. Affinity window model of self-MHC selection. Hypothetical distribution of affinities (K_d) for a given MHC determinant and a selection "window" which might determine which T cells migrate to the periphery (see text).

Case 1:06-cv-00500-SLR-MPT Document 270 Filed 08/28/2008 Page 35 of 41

The material on this page was copied from the collection of the National Library of Medicine by a third party and may be protected by U.S. Copyright law.

Kd, more on the order of immunoglobulin which is in the 10^{-6}–10^{-10} range). This tighter binding might then trigger that particular T cell to clonal expansion. In this "affinity window" model, cells bearing receptors which bind tightly to self-MHC (which would be deleterious) would be eliminated, whereas those with too low an affinity would have many more chances at other determinants. Additionally, evolutionary pressures would pre-select for variable region components which are adaptable to class I and class II determinants to lower the attrition rate and to account for the large number of alloreactive cells.

SUMMARY

We describe here our efforts to develop a systematic strategy for the enumeration and isolation of genes encoding T cell-specific, membrane-associated polypeptides. Of particular importance among the cDNA clones that we have isolated is one which encodes the beta chain of the murine T cell receptor for antigen. The gene product is strikingly similar to immunoglobulin in its variable (V), constant (C), joining (J), and diversity (D) – like elements and the ability of the latter three types of element to assort independently during differentiation. The genomic organization of the constant region locus which encodes this molecule consists of two tandemly arrayed units of the form JC/JC, where the J clusters consist of fourteen distinct elements, many of which may be functional. The two constant regions differ by only four amino acids and both are apparently expressed in T cells of the same phenotype, so they probably do not represent isotypes in the classical sense. The sequences flanking the V, D and J elements are also similar to the conserved heptamer and nonomer sequences of immunoglobulins thought to be important in the recombination of the specific gene segments. These similarities indicate both the common evolutionary origins of these loci and the strong selective pressure that must be operative. The T cell receptor locus differs somewhat from immunoglobulins in the large number of possible J region elements and to some extent in the hypervariable-framework regions of the V region. We and others have mapped this gene to chromosone 6 of the mouse, in the same portion of the chromosome but not closely linked the kappa locus. The significance of the predicted protein structure of the beta chain and its support of the one-receptor model of MHC-antigen recognition are discused.

ACKNOWLEDGEMENTS

This work was supported, in part, by grants to M.M.D. from the National Institutes of Health (AI19512 and AI20320) and from the American Cancer Society (IM00364) and to S.M.H. from the Cancer Foundation. N.R.J.G. is a fellow of the Cancer Research Institute of New York. We wish to thank Kathleen Redman for expert secretarial assistance, Phil Patten for helpful discussions, and David Cohen for critical reading of the manuscript.

REFERENCES

Acuto, O., Hussey, R. E., Fitzgerald, K. A., Protentis, J. P., Meuer, S. C., Schlossman, S. F. & Reinherz, E. L. (1983a) The human T cell receptor: Appearance in ontogeny and biochemical relationship of α and β subunits on IL-2 dependent clones and T cell tumors. *Cell* 34, 717.

Acuto, O., Meuer, S. C., Hodgdon, J. C., Schlossman, S. F. & Reinherz, E. L. (1983b) Peptide variability exists within α and β subunits of the T cell receptor for antigen. *J. Exp. Med.* 158, 1368.

Acuto, O., Fabbi, M., Smart, J., Poole, C. B., Protentis, J., Royer, H.-D., Schlossman, S. & Reinherz, E. L. (1984) Purification and N-terminal amino acid sequence of the β subunit of a human T cell antigen receptor. *Proc. Natl. Acad. U.S.A.* (in press).

Allison, J. P., MacIntyre, B. W. & Block, D. (1982) Tumor specific antigen and murine T-lymphoma defined with monoclonal antibody. *J. Immunol.* 129, 2293.

Amzel, L. M., Poljak, R. J., Saul, F., Varga, J. M. & Richards, F. F. (1974) The three dimensional structure of a combining region-ligand complex of immunoglobulin NEW at 3.5-A resolution. *Proc. Natl. Acad. Sci. U.S.A.* 71, 1427.

Binz, H., Wigzell, H. & Bazin, H. (1976) T-cell idiotypes are linked to immunoglobulin heavy chain genes. *Nature* 264, 639.

Cayre, Y., Palladino, M. A., Marcu, K. B. & Stavnezer, J. (1981) Expression of an antigen receptor on T cells does not require recombination at the immunoglobulin J_H-Cμ locus. *Proc. Natl. Acad. Sci. U.S.A.* 78, 3814.

Chien, Y., Gascoigne, N. R. J., Kavaler, J., Lee, N. E. & Davis, M. M. (1984) Somatic recombination in a murine T cell receptor gene. *Nature* 309, 322.

Coutinho, A. & Meo, T. (1983) Immunoglobulin gene expression by T lymphocytes. *Scand. J. Immunol.* 18, 79.

Crampton, J., Humphries, S., Woods, D. & Williamson, R. (1980) The isolation of cloned cDNA sequences which are differentially expressed in human lymphocytes and fibroblasts. *Nucleic Acids Research* 8, 6007.

Davies, D. R., Padlan, E. A. & Segal, D. M. (1975) Three-dimensional structure of immunoglobulins. *Ann. Rev. Biochem.* 44, 639.

Davis, M. M., Cohen, D. I., Nielsen, E. A., DeFranco, A. D. & Paul, W. E. (1982) The isolation of B and T cell specific genes. In: *B and T Cell Tumors* (UCLA Symposia) (E. Vitetta & C. F. Fox, eds.) Vol. 24, p. 215. Academic Press, New York.

Davis, M. M., Cohen, D. I., Nielsen, E. A., Steinmetz, M., Paul, W. E. & Hood, L. (1984) Cell-type specific cDNA probes and the murine I region: The localization and orientation of A^d_a. *Proc. Natl. Acad. Sci. U.S.A.* 81, 2194.

Dworkin, M. B. & David, I. B. (1980) Construction of a cloned library of expressed embryonic gene sequences from *Xenopus laevis*. *Develop. Biol.* 76, 435.

Early, P., Huang, H., Davis, M., Calame, K. & Hood, L. (1980a) An immunoglobulin heavy chain variable region gene is generated from three segments of DNA: V_H, D and J_H. *Cell* 19, 981.

Early, P., Rogers, J., Davis, M., Calame, K., Bond, M., Wall, R. & Hood, L. (1980b) Two mRNAs can be produced from a single immunoglobulin μ gene by alternative RNA processing pathways. *Cell* 20, 313.

Epstein, R., Roehm, Cohn, M., Marrack, P., Kappler, J., Davis, M. & Hedrick, S. in prep.

Fathman, C. G. & Frelinger, J. G. (1983) T-lymphocyte clones. *Ann. Rev. Immunol.* 1, 633.

Case 1:06-cv-00500-SLR-MPT Document 270 Filed 08/28/2008 Page 36 of 41

The material on this page was copied from the collection of the National Library of Medicine by a third party and may be protected by U.S. Copyright law.

Gasc N. R. J., Chien, Y., Becker, D. M., Kavaler, J. & Davis, M. M. (1984) Genomic o.g anisation and sequence of T cell receptor constant and joining region genes. *Nature* 310, 421.

Haskins, K., Kubo, R., White, J., Pigeon, M., Kappler, J. & Marrack, P. (1983) The major histocompatibility complex-restricted antigen receptor on T cells. I. Isolation with a monoclonal antibody. *J. Exp. Med.* 157, 1149.

Heber-Katz, E., Schwartz, R. H., Matis, L. A., Hannum, C., Fairwell, T., Appella, E. & Hansburg, D. (1982) Contribution of antigen-presenting cell major histocompatibility complex gene products to the specificity of antigen-induced T cell activation. *J. Exp. Med.* 155, 1086.

Hedrick, S. M., Cohen, D. I., Nielsen, E. A. & Davis, M. M. (1984a) The isolation of cDNA clones encoding T cell-specific membrane-associated proteins. *Nature* 308, 149.

Hedrick, S. M., Nielsen, E. A., Kavaler, J., Cohen, D. I. & Davis, M. M. (1984b) Sequence relationships between putative T-cell receptor polypeptides and immunoglobulins. *Nature* 308, 153.

Hedrick, S. M., Germain, R. N., Bevan, M. J., Dorf, M., Fink, P., Gascoigne, N. R. J., Greene, M., Kapp, J., Kauffman, Y., Melchers, F., Pierce, C., Sorensen, C., Taniguichi, M. & Davis, M. M. (1984c) Expression of the T cell receptor β chain in T lymphocyte subsets. (Manuscript in preparation).

Hood, L., Davis, M., Early, P., Calame, K., Kim, S., Crews, S. & Huang, H. (1980) Two types of DNA rearrangements in immunoglobulin genes. *Cold Spring Harbor Symp. Quant. Biol.* 45, 887.

Infante, A. J., Infante, P. D., Gillis, S. & Fathman, C. G. (1982) Definition of T cell idiotypes using anti-idiotypic antisera produced by immunization with T cell clones. *J. Exp. Med.* 155, 1100.

Jerne, N. K. (1971) The somatic generation of immune recognition. *Eur. J. Immunol.* 1, 1.

Kabat, E. A., Wu, T. T., Bilofsky, H., Reid-Miller, M. & Perry, H. (1983) *Sequences of immunological interest.* U.S. Dept. of Health and Human Services, Washington, D.C.

Kappler, J., Kubo, R., Haskins, K., Hannum, C., Marrack, P., Pigeon, M., McIntyre, B., Allison, J. & Trowbridge, I. (1983) The major histocompatibility complex-restricted antigen receptor on T cells in mouse and man: Identification of constant and variable peptides. *Cell* 35, 295.

Kappler, J., Skidmore, B., White, J. & Marrack, P. (1981) Antigen inducible, H-2 restricted, interleukin-2-producing T cell hybridomas. Lack of independent antigen and H-2 recognition. *J. Exp. Med.* 153, 1198.

Kavaler, J., Davis, M. M. & Chien, Y. (1984) Isolation of a T cell receptor Diversity (D) region element. *Nature* 310, 421.

Kaye, J., Porcelli, S., Tite, J., Jones, B. & Janeway, C. A. (1983) Both a monoclonal antibody and antisera specific for determinants unique to individual cloned helper T cell lines can substitute for antigen and antigen-presenting cells in the activation of T cells. *J. Exp. Med.* 158, 836.

Kaye, J. & Joneway, C. A. (1984) Glycosylation of murine T cell receptor α and β chains. *J. Immunol.* in press.

Kemp, D. J., Harris, A. W., Cory, S. & Adams, J. M. (1980) Expression of the immunoglobulin $C\mu$ in mouse T and B lymphoid and myeloid cell lines. *Proc. Natl. Acad. Sci. U.S.A.* 77, 2876.

Kraig, E., Kronenberg, M., Kapp, J. A., Pierce, C. W., Abruzzini, A. F., Sorensen, C. M., Samelson, L. E., Schwartz, R. H. & Hood, L. E. (1983) T and B cells that recognize the same antigen do not transcribe similar heavy chain variable region gene segments. *J. Exp. Med.* 158, 192.

Kronenberg, M., Davis, M. M., Early, P. W., Hood, L. E. & Watson, J. D. (1980) Helper and killer T cells do not express B cell immunoglobulin joining and consta .on gene segments. *J. Exp. Med.* 152, 1745.

Kronenberg, M., Kraig, E., Siu, G., Kapp, J. A., Kappler, J., Marrack, P., Pierce, C. W. & Hood, L. (1983) Three T-cell hybridomas do not contain detectable heavy chain variable region transcripts. *J. Exp. Med.* 158, 210.

Kurosawa, Y. & Tonegawa, S. (1982) Organization, structure, and assembly of immunoglobulin heavy chain diversity DNA segments. *J. Exp. Med.* 155, 201.

Lee, N. E., D'Eustachio, P., Pratcheva, D., Ruddle, F., Hedrick, S. M. & Davis, M. M. (1984) One chain of the murine T cell receptor is encoded on chromosome six. *J. Exp. Med.*, in press.

Lewin, B. (1980) In: *Gene Expression II.* 2nd edn. Wiley, New York.

Matzinger, P. (1981) A one-receptor view of T-cell behavior. *Nature* 292, 497.

Max, E. E., Seidman, J. G. & Leder, P. (1979) Sequence of five potential recombination sites encoded close to an immunoglobulin κ constant region gene. *Proc. Natl. Acad. Sci. U.S.A.* 76, 3450.

McCartney-Francis, N., Skuria, R. M., Mage, R. G. & Bernstein, K. E. (1984) K-chain allotypes and isotypes in the rabbit: cDNA sequences of clones encoding b9 suggest an evolutionary pathway and possible role of the interchain disulfide bond in quantitative allotype expression. *Proc. Natl. Acad. Sci. USA* 81, 1794.

McIntyre, B. W. & Allison, J. P. (1983) The mouse T cell receptor: Structural heterogeneity of molecules of normal T cells defined by xenoantiserum. *Cell* 34, 739.

Mechler, B. & Rabbitts, T. M. (1981) Membrane-bound ribosomes of myeloma cells IV. mRNA complexity of free and membrane-bound polysomes. *J. Cell Biol.* 88, 29.

Meuer, S. C., Fitzgerald, K. A., Hussey, R. E., Hodgdon, J. C., Schlossman, S. F. & Reinherz, E. L. (1983) Clonotypic structures involved in antigen-specific human T cell function. Relationship to the T3 molecular complex. *J. Exp. Med.* 157, 705.

Moriuchi, T., Chang, H. C., Denome, R. & Silver, J. (1983) thy-1 cDNA sequence suggests a novel regulatory mechanism. *Nature* 301, 80.

Nakanishi, K., Sugimura, K., Yaoita, Y., Maeda, K., Kashiwamura, S., Honjo, T., & Kishimoto, T. (1982) A T15-idiotype-positive T suppressor hybridoma does not use the T15 V_H gene segment. *Proc. Natl. Acad. Sci. U.S.A.* 79, 6984.

Owen, F. L. & Riblet, R. (1984) Genes for the mouse T cell alloantigens T_{gic}, T_{thy}, T_{lad}, and T_{tu} are closely linked near IgH on chromosome 12. *J. Exp. Med.* 159, 313.

Rajewsky, K. & Eichmann, K. (1977) Antigen receptors of T helper cells. *Contemp. Top. Immunobiol.* 7, 69.

Sakano, H., Huppi, K., Heinrich, G. & Tonegawa, S. (1979) Sequences at the somatic recombination sites of immunoglobulin light-chain genes. *Nature* 280, 288.

Sakano, H., Kurosawa, Y., Weigert, M. & Tonegawa, S. (1981) Identification and nucleotide sequence of a diversity DNA segment (D) of immunoglobulin heavy-chain genes. *Nature* 290, 562.

Samelson, L. E., Germain, R. N. & Schwartz, R. H. (1983) Monoclonal antibodies against the antigen receptor on a cloned T-cell hybrid. *Proc. Natl. Acad. Sci. U.S.A.* 80, 6972.

Shen-Ong, G. L. C., Keath, E. J., Piccoli, S. P. & Cole, M. D. (1982) Novel myc oncogene RNA from abortive immunoglobulin-gene recombination in mouse plasmacytomas. *Cell* 31, 443.

Sherman, L. A., Vitiello, A. & Klinman, N. (1983) T-cell and B-cell responses to viral antigens at the clonal level. *Ann. Rev. Immunol.* 1, 63.

Siu, G., Clarke, S. P., Yoshikai, Y., Malissen, M., Yanagi, Y., Strauss, E., Mak, T. W. & Hood, L. (1984) The human T cell receptor is encoded by variable, diversity, and joining gene segments that rearrange to generate a complete V gene. *Cell* 37, 393.

Staerz, U. D., Pasternack, M. S., Klein, J. R., Benedetto, J. D. & Bevan, M. J. (1984)

Case 1:06-cv-00500-SLR-MPT Document 270 Filed 08/28/2008 Page 37 of 41

The material on this page was copied from the collection of the National Library of Medicine by a third party and may be protected by U.S. Copyright law.

Monoclonal antibodies specific for a murine cytotoxic T-lymphocyte clone. *Proc. Natl. Acad. Sci. USA* 81, 1799.
Terhorst, C. (1984) Cell surface structures involved in human T lymphocyte specific functions: analysis with monoclonal antibodies. In: *Antibodies to Receptors: Probes for Receptor Structure and Function* (M. E. Greaves, ed.). Chapman and Hall, London (in press).
Tonegawa, S. (1983) Somatic generation of antibody diversity. *Nature* 302, 575.
Wilbur, N. J. & Lipman, D. J. (1983) Rapid similarity searches of nucleic acid and protein data banks. *Proc. Natl. Acad. Sci. U.S.A.* 80, 726.
Williams, A. F. (1984) The T-lumphocyte antigen receptor: elusive no more. *Nature* 308, 108.
Williamson, A. R. (1980) Three-receptor, clonal expansion model for selection of self-recognition in the thymus. *Nature* 283, 527.
Wu, T. T. & Kabat, E. A. (1970) An analysis of the sequences of the variable regions of Bence Jones proteins and myeloma light chains and their implications for antibody complementarity. *J. Exp. Med.* 132, 211.
Yanagi, Y., Yoshikai, Y., Leggett, K., Clark, S. P., Aleksander, I. & Mak, T. W. (1984) A human T cell-specific cDNA clone encodes a protein having extensive homology to immunoglobulin chains. *Nature* 308, 145.

Case 1:06-cv-00500-SLR-MPT Document 270 Filed 08/28/2008 Page 38 of 41

The material on this page was copied from the collection of the National Library of Medicine by a third party and may be protected by U.S. Copyright law.

Exhibit 12
Redacted In Its Entirety

UNITED STATES DISTRICT COURT
FOR THE DISTRICT OF DELAWARE

CERTIFICATE OF SERVICE

I hereby certify that on August 25, 2008, I electronically filed the foregoing document with the Clerk of the Court using CM/ECF which will send notification of such filing to the following and which has also been served as noted:

BY HAND DELIVERY AND E-MAIL

Philip A. Rovner
Potter, Anderson & Corroon
Hercules Plaza - 6th Floor
Wilmington, DE 19899

I hereby certify that on August 25, 2008, the foregoing document was sent to the following non-registered participants in the manner indicted:

BY E-MAIL

Paul J. Andre
King & Spalding, LLP
1000 Bridge Parkway
Suite 100
Redwood Shores, CA 94065

/s/ Kelly E. Farnan
Kelly E. Farnan (#4395)

UNITED STATES DISTRICT COURT
FOR THE DISTRICT OF DELAWARE

CERTIFICATE OF SERVICE

I hereby certify that on August 28, 2008, I electronically filed the foregoing document with the Clerk of the Court using CM/ECF which will send notification of such filing to the following and which has also been served as noted:

BY HAND DELIVERY

Philip A. Rovner
Potter, Anderson & Corroon
Hercules Plaza - 6th Floor
Wilmington, DE 19899

BY FEDERAL EXPRESS

Paul J. Andre
King & Spalding, LLP
1000 Bridge Parkway
Suite 100
Redwood Shores, CA 94065

Kelly E. Farnan (#4395)